![JEM Journal of Experimental Medicine logo]

ARTICLE

Nucleoside-modified mRNA vaccines induce potent T follicular helper and germinal center B cell responses

Norbert Pardi[1], Michael J. Hogan[1], Martin S. Naradikian[2], Kaela Parkhouse[3], Derek W. Cain[4], Letitia Jones[4], M. Anthony Moody[4], Hans P. Verkerke[5], Arpita Myles[2], Elinor Willis[3], Celia C. LaBranche[6], David C. Montefiori[6], Jenna L. Lobby[7], Kevin O. Saunders[4], Hua-Xin Liao[4], Bette T. Korber[8], Laura L. Sutherland[4], Richard M. Scearce[4], Peter T. Hraber[8], István Tombácz[1], Hiromi Muramatsu[1], Houping Ni[1], Daniel A. Balikov[1], Charles Li[1], Barbara L. Mui[9], Ying K. Tam[9], Florian Krammer[10], Katalin Karikó[11], Patricia Polacino[12], Laurence C. Eisenlohr[7], Thomas D. Madden[9], Michael J. Hope[9], Mark G. Lewis[13], Kelly K. Lee[5], Shiu-Lok Hu[12,14], Scott E. Hensley[3], Michael P. Cancro[2], Barton F. Haynes[4], and Drew Weissman[1]

T follicular helper (Tfh) cells are required to develop germinal center (GC) responses and drive immunoglobulin class switch, affinity maturation, and long-term B cell memory. In this study, we characterize a recently developed vaccine platform, nucleoside-modified, purified mRNA encapsulated in lipid nanoparticles (mRNA-LNPs), that induces high levels of Tfh and GC B cells. Intradermal vaccination with nucleoside-modified mRNA-LNPs encoding various viral surface antigens elicited polyfunctional, antigen-specific, CD4+ T cell responses and potent neutralizing antibody responses in mice and nonhuman primates. Importantly, the strong antigen-specific Tfh cell response and high numbers of GC B cells and plasma cells were associated with long-lived and high-affinity neutralizing antibodies and durable protection. Comparative studies demonstrated that nucleoside-modified mRNA-LNP vaccines outperformed adjuvanted protein and inactivated virus vaccines and pathogen infection. The incorporation of noninflammatory, modified nucleosides in the mRNA is required for the production of large amounts of antigen and for robust immune responses.

Introduction

Protective immunity against many pathogens can be achieved through long-lived and high-affinity antibody responses, which are driven by T follicular helper (Tfh) cells. Tfh cells are required for the formation and maintenance of germinal centers (GCs), in which B cell affinity maturation, class switch, and development of long-lived plasma and memory B cells occur (Victora and Nussenzweig, 2012; Crotty, 2014). Tfh cells drive affinity maturation through successive rounds of somatic hypermutation and selection, which is required to develop broadly protective responses against many pathogens, including HIV and influenza virus (Kwong and Mascola, 2012; Kwong et al., 2013; Yamamoto et al., 2015; Krammer, 2016). Thus, the magnitude or quality of antibody responses induced by a vaccine is shaped by its ability to induce Tfh cells. The identification of vaccine platforms or adjuvants that specifically induce potent Tfh cell responses has been recognized as a critical need in vaccinology (Havenar-Daughton et al., 2017).

Nucleic acid–based vaccines were first described over two decades ago (Martinon et al., 1993) and have been extensively studied for infectious pathogens (Villarreal et al., 2013). The majority of investigations focused on DNA-based vaccines because of concerns about mRNA instability and the inefficient in vivo delivery. In recent years, most of those concerns have been resolved by rapid advancements in technology, and in vitro–transcribed mRNA has become a promising candidate for vaccine development (Pardi et al., 2018). Compared with other nucleic acid–based systems, mRNA combines several positive attributes, including lack of integration into the host genome, translation in both dividing and nondividing cells, and immediate protein production for a controllable amount of time.

To develop a potent vaccine with mRNA-encoded antigens, it was important to improve the translatability and stability of the mRNA and the efficiency of its in vivo delivery. Thus, various modifications have been introduced, including cap1 addition, efficient 5′ and 3′ untranslated regions, codon-optimized coding sequences, and a long poly(A) tail. Further improvements in protein translation have been achieved by eliminating pathogen-associated molecular patterns in mRNA via incorporation of modified nucleosides, such as pseudouridine (Karikó et al., 2008) and 1-methylpseudouridine (m1Ψ; Andries et al., 2015), and fast protein liquid chromatography (FPLC) purification to remove double-stranded RNA contaminants (Karikó et al., 2011). A wide variety of carrier formulations have been developed to protect mRNA from degradation and facilitate uptake into cells (Kauffman et al., 2016). Of these, lipid nanoparticles (LNPs; Morrissey et al., 2005) have proven to mediate highly efficient and prolonged protein expression in vivo, particularly after intradermal (i.d.) delivery (Pardi et al., 2015).

In recent years, several RNA-based vaccines have been developed against infectious diseases, using various delivery mechanisms, adjuvants, and in some cases, self-replicating RNAs (Pardi et al., 2018). Our laboratory recently described an effective vaccine against Zika virus (ZIKV) using FPLC-purified, m1Ψ-modified mRNA encapsulated in LNPs (m1Ψ–mRNA-LNPs). A single, low-dose immunization with m1Ψ-mRNA–LNPs encoding the ZIKV premembrane and envelope (prM-E) surface proteins elicited rapid and durable protective immune responses in mice and rhesus macaques (Pardi et al., 2017). A similar vaccine using m1Ψ-mRNA-LNPs was shown to protect mice from ZIKV infection after two immunizations (Richner et al., 2017). Recent publications demonstrated that mRNA-LNP vaccination against influenza virus resulted in potent immune responses in multiple animal species and humans (Bahl et al., 2017; Liang et al., 2017; Lindgren et al., 2017; Lutz et al., 2017).

In this study, we characterize the immunogenicity of three vaccines consisting of m1Ψ-modified, FPLC-purified mRNA-LNPs encoding HIV-1 envelope (Env), ZIKV prM-E, and influenza virus hemagglutinin (HA), which induce remarkably potent and durable neutralizing antibody responses. Importantly, we show that this enhanced neutralizing activity follows robust induction of Tfh and GC B cells. Furthermore, we demonstrate that mRNA-LNPs act as highly effective adjuvants and that incorporation of the modified-nucleoside m1Ψ is essential for high and sustained protein production from mRNA-LNPs, which was associated with potent Tfh and B cell responses.

Results
Delivery (i.d.) of m1Ψ-mRNA-LNPs results in efficient protein production for an extended period of time
A great variety of antigen-presenting cells reside in the skin (Clausen and Stoitzner, 2015), making it an ideal site for immunogen delivery during vaccination. Firefly luciferase (Luc)–encoding m1Ψ-mRNA–LNPs administered to mice by the i.d. route were translated at a high level compared with naked (uncomplexed) mRNA and showed a gradual decrease in protein expression over 13 d (Fig. 1, A–C), which are favorable kinetics for immunization,

mimicking live-virus delivery systems. Nucleoside modification was necessary for this high level of protein production: replacement of uridine (U) with m1Ψ resulted in ~20 times more total luciferase protein and a longer duration of measurable protein expression after i.d. mRNA-LNP injection (Fig. 1, D–F).

m1Ψ-mRNA–LNP vaccination induces strong antigen-specific T cell responses
BALB/c mice were injected i.d. with increasing amounts (3, 10, and 30 µg) of m1Ψ-mRNA–LNPs encoding a variant of clade B HIV-1 R3A Env (Meissner et al., 2004) or Luc, at weeks 0 and 4. At week 6, antigen-specific T cell responses were determined. High frequencies of antigen-specific CD4+ T cells expressing IFN-γ, TNF-α, and IL-2 were measured in Env mRNA–vaccinated animals (Fig. 2, A–C and Fig. S1 A). The lowest dose of mRNA (3 µg) elicited the highest CD4+ T cell responses, although the difference was not significant. Notably, many of the antigen-specific CD4+ T cells were polyfunctional, producing multiple cytokines (Fig. 2 D).

To determine whether similar results were obtained with a different immunogen, a single dose of 30 µg of m1Ψ-mRNA–LNPs encoding HA from influenza A/Puerto Rico/8/1934 (PR8; H1N1, mouse adapted) or Luc was administered to mice, and CD4+ T cell responses were examined 10 d after immunization. Strong antigen-specific CD4+ T cell responses were measured in splenocytes of all mice vaccinated with HA m1Ψ-mRNA–LNPs (Fig. 3, A–C; and Fig. S1 A). Mice that received an intramuscular (i.m.) injection of 1,000 hemagglutinating units (HAUs) of inactivated PR8 influenza virus, a viral particle-based vaccine (Quan et al., 2016), generated comparatively weak CD4+ T cell responses (Fig. 3). As observed with two immunizations, a large fraction of the antigen-specific CD4+ T cells in the m1Ψ-mRNA-LNP–injected mice were polyfunctional (Fig. 3 D).

Antigen-specific CD8+ T cell responses were investigated in mice immunized with two doses of Env-encoding m1Ψ-mRNA-LNPs. Strong Env-specific, CD8+ T cell responses were detected for the 3 and 10 µg doses, with significant generation of polyfunctional CD8+ T cells expressing IFN-γ, TNF-α, and CD107a (Fig. 4). Interestingly, CD8+ T cell responses were less pronounced in animals that were injected with 30 µg of m1Ψ-mRNA-LNPs.

m1Ψ-mRNA-LNP immunization induces potent and durable antibody responses in mice
Serum from mice immunized twice with 3, 10, or 30 µg of HIV Env-encoding m1Ψ-mRNA-LNPs was collected 2 wk after the second immunization, and the humoral immune response was evaluated. High levels of anti–gp120 IgG (~24 µg/ml) were obtained in mice injected with 10 or 30 µg of Env m1Ψ-mRNA-LNPs (Fig. S2). In comparison, two immunizations with 3 µg of m1Ψ-mRNA-LNPs resulted in ~20-fold lower anti–gp120 antibody levels (Fig. S2), despite robust CD4+ T cell responses (Fig. 2).

Neutralizing antibodies that block influenza virus attachment to sialic acid can be measured with a hemagglutination inhibition (HAI) assay. An in vitro HAI titer of 1:40 is considered the correlate of in vivo protection from influenza infection in humans (Hannoun et al., 2004). After a single immunization in mice with 30 µg of PR8 HA m1Ψ-mRNA-LNPs, HAI titers of ~1:640 were observed at 2 wk (Fig. 5 A), which increased to
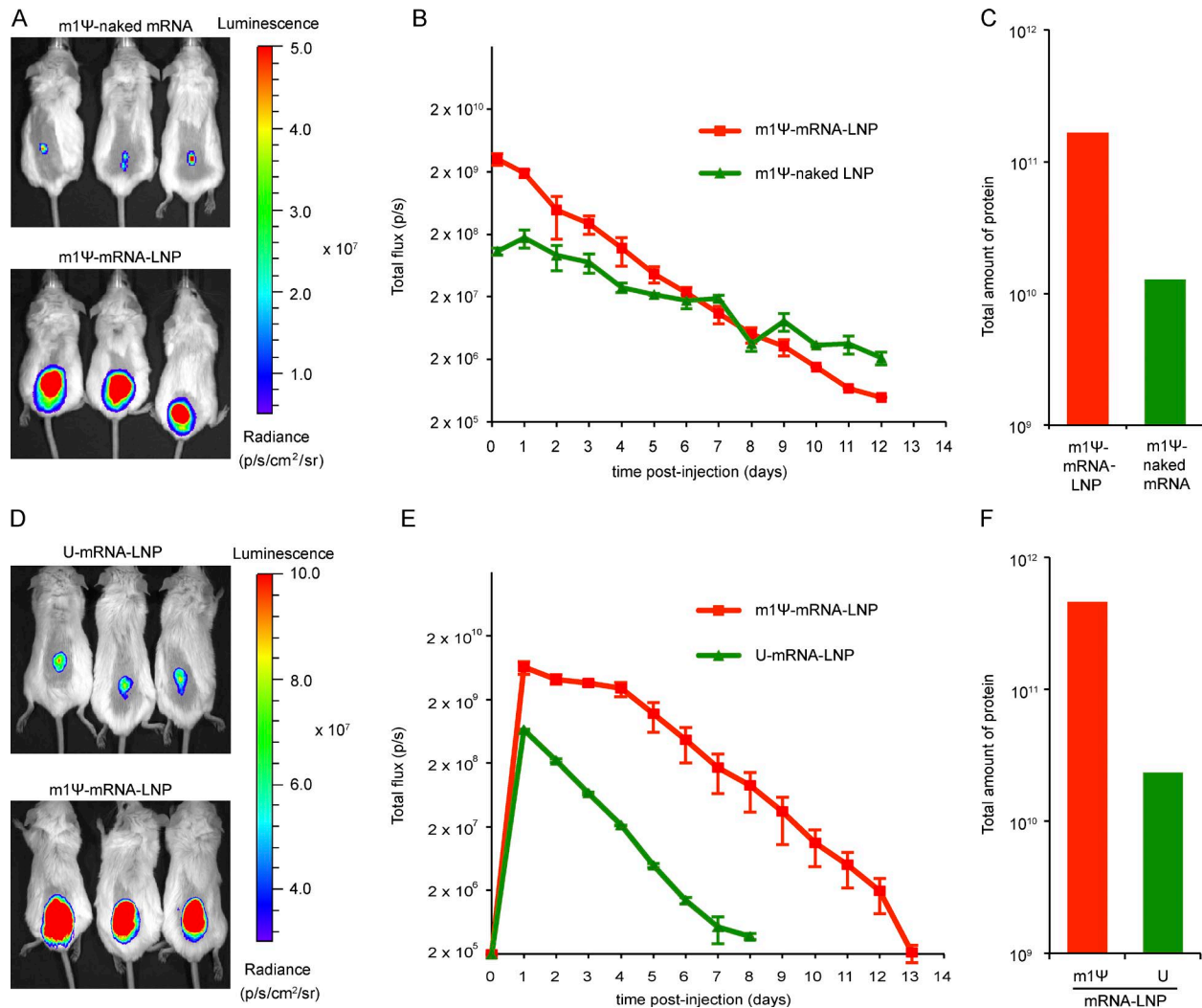
Pardi et al.
Modified mRNA vaccines induce Tfh and GC B cells

Journal of Experimental Medicine
https://doi.org/10.1084/jem.20171450

1572

Figure 1. **m1Ψ-mRNA-LNPs are translated at higher levels than naked m1Ψ-mRNAs or U-mRNA-LNPs in mice. (A)** Representative IVIS image (4 h after injection) of BALB/c mice i.d. injected with 5.0 µg of naked (uncomplexed) or LNP-complexed Luc m1Ψ-mRNA. **(B)** Quantitation of the bioluminescent signal measured after delivery of mRNA over time. **(C)** Total amount of protein produced from the mRNA over time. **(D)** Representative IVIS image (24 h after injection) of BALB/c mice i.d. injected with 5.0 µg of Luc U- or m1Ψ-mRNA-LNPs. **(E)** Quantitation of the bioluminescent signal measured over time after delivery of mRNA-LNPs. **(F)** Total amount of protein produced from Luc U- or m1Ψ-mRNA-LNPs over time. Area under the curve was calculated as described in the Materials and methods section. Error bars are SEM.

~1:2,000 at 4 wk (Fig. 5 B). As a comparison, immunization with inactivated PR8 virus resulted in >40-fold lower HAI titers (Fig. 5, A and B), and intranasal inoculation of live PR8 virus, i.e., pathogenic infection, elicited significantly lower HAI titers than a single nucleoside-modified mRNA-LNP vaccination (Fig. 5, A and B).

Immune responses against HIV-1 and influenza vaccines have been characterized by poor durability of the antigen-specific serum antibody response (Montefiori et al., 2012; Krammer, 2016). HAI titers in mice immunized with a single dose of HA m1Ψ-mRNA-LNPs were followed over time and were found to be stable for at least 13 mo after immunization (Fig. 5 C). HA and Luc m1Ψ-mRNA-LNP–immunized mice were infected with a lethal dose of PR8 influenza virus 13 mo after vaccination. All animals in the Luc control group lost weight and reached protocol termination criteria, whereas all HA mRNA–immunized animals survived virus infection without weight loss (Fig. 5, D and E),

demonstrating that nucleoside-modified mRNA-LNP immunization elicited durable protective immunity.

Immunization with m1Ψ-mRNA-LNPs expands GC B cells
The GC reaction allows B lymphocytes to proliferate, class switch, undergo affinity maturation, and differentiate into long-lived plasma and memory cells (Victora and Wilson, 2015). The potency and longevity of antibody responses elicited by m1Ψ-mRNA-LNPs were characteristic of efficient GC reactions. Accordingly, total splenic GC B cells, (IgM$^-$, IgD$^-$, B220$^+$, CD19$^+$, CD138$^-$, CD38^{low}, and peanut agglutinin high [PNA^{high}]), were massively increased (~10–20-fold) after a single immunization with 30 µg of PR8 HA m1Ψ-mRNA-LNPs compared with naive controls and mice immunized with Luc m1Ψ-mRNA-LNPs, inactivated PR8 virus, or MF59-adjuvanted recombinant PR8 HA protein (Figs. S1 B and S3 A). Of note, live PR8 virus immunization resulted in comparably potent GC B cell proliferation, likely
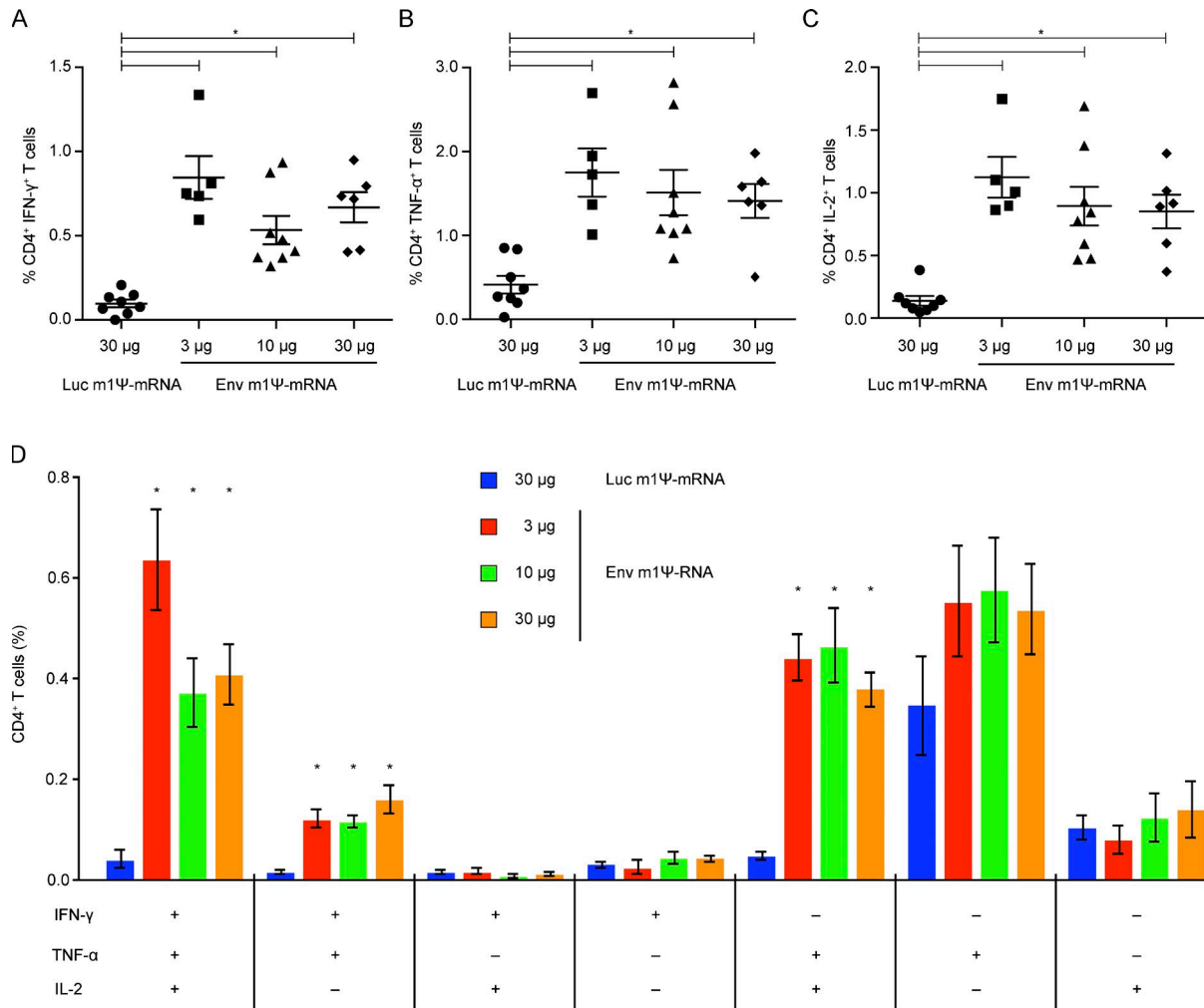
Pardi et al.
Modified mRNA vaccines induce Tfh and GC B cells

Journal of Experimental Medicine
https://doi.org/10.1084/jem.20171450

1573

Figure 2. **Two immunizations with HIV-1 Env m1Ψ-mRNA-LNPs elicit potent antigen-specific CD4+ T cell responses.** Mice received i.d. immunizations of Luc or HIV Env m1Ψ-mRNA-LNPs at weeks 0 and 4. Splenocytes were stimulated with Env peptides 2 wk after the second immunization, and cytokine production by CD4+ T cells was assessed by flow cytometry. **(A–C)** Percentages of CD4+ T cells producing IFN-γ (A), TNF-α (B), and IL-2 (C) are shown. **(D)** Frequencies of combinations of cytokines produced by CD4+ T cells. n = 5–8 mice, and each symbol represents one animal. Experiments were repeated at least two times to achieve statistical significance. Error bars are SEM. Statistical analysis: (A–C) one-way ANOVA with Bonferroni correction, *, $P < 0.05$; (D) Student's t test, *, $P < 0.05$ compared with Luc mRNA–immunized mice.

directed at multiple influenza virus antigens. The lack of a GC B cell response, which was measured in an antigen-nonspecific manner, to Luc mRNA-LNP vaccination may be due to its intracellular expression preventing efficient activation of the B cells. The numbers of splenic plasma cells were also increased 10 d after a single immunization relative to naive mice and mice that received Luc mRNA-LNPs, inactivated PR8 virus, live PR8 virus, or MF59-adjuvanted recombinant PR8 HA protein (Fig. S3 B). Although the B cell responses were characterized at the predicted peak of the GC at d 10, it is not currently known how the kinetics of the GC reaction differ in these various vaccine formats and whether this may affect downstream immune responses.

m1Ψ-mRNA-LNP vaccination induces strong antigen-specific Tfh cell responses

Because the m1Ψ-mRNA-LNP vaccine platform elicited strong CD4+ T cell responses, massive GC B cell activation, and potent and long-lived antibody responses, total and antigen-specific Tfh

cell induction was analyzed. In mice, a single i.d. dose of 30 μg of HA m1Ψ-mRNA-LNPs significantly increased the total number of Tfh cells in spleen (Fig. 6 A and Fig. S1 C). Of note, live PR8 virus immunization resulted in higher numbers of splenic Tfh cells, although their specificity is not known because the influenza virus produces 10 different proteins. Gene-expression analysis in purified splenic Tfh cells demonstrated characteristic increases in IFN-γ, IL-4, and IL-21 mRNA transcript levels after HA m1Ψ-mRNA-LNP immunization (Fig. 6 B). Elevated numbers of CD4+ Bcl6+IFN-γ+ splenic Tfh-like cells, induced by peptide stimulation, were detected after immunization with a single dose of 30 μg of HA or Env m1Ψ–modified mRNA-LNPs (Fig. 6, C and D).

As Tfh cells promote affinity maturation, the apparent affinity of the polyclonal response after m1Ψ-modified influenza HA mRNA-LNP immunization was measured 2, 4, and 8 wk after a single immunization in mice (Fig. 6 E and Fig. S4 A). An average dissociation constant of 362 pM was measured 2 wk after immunization, which decreased to 75 pM at 4 wk. A trend toward
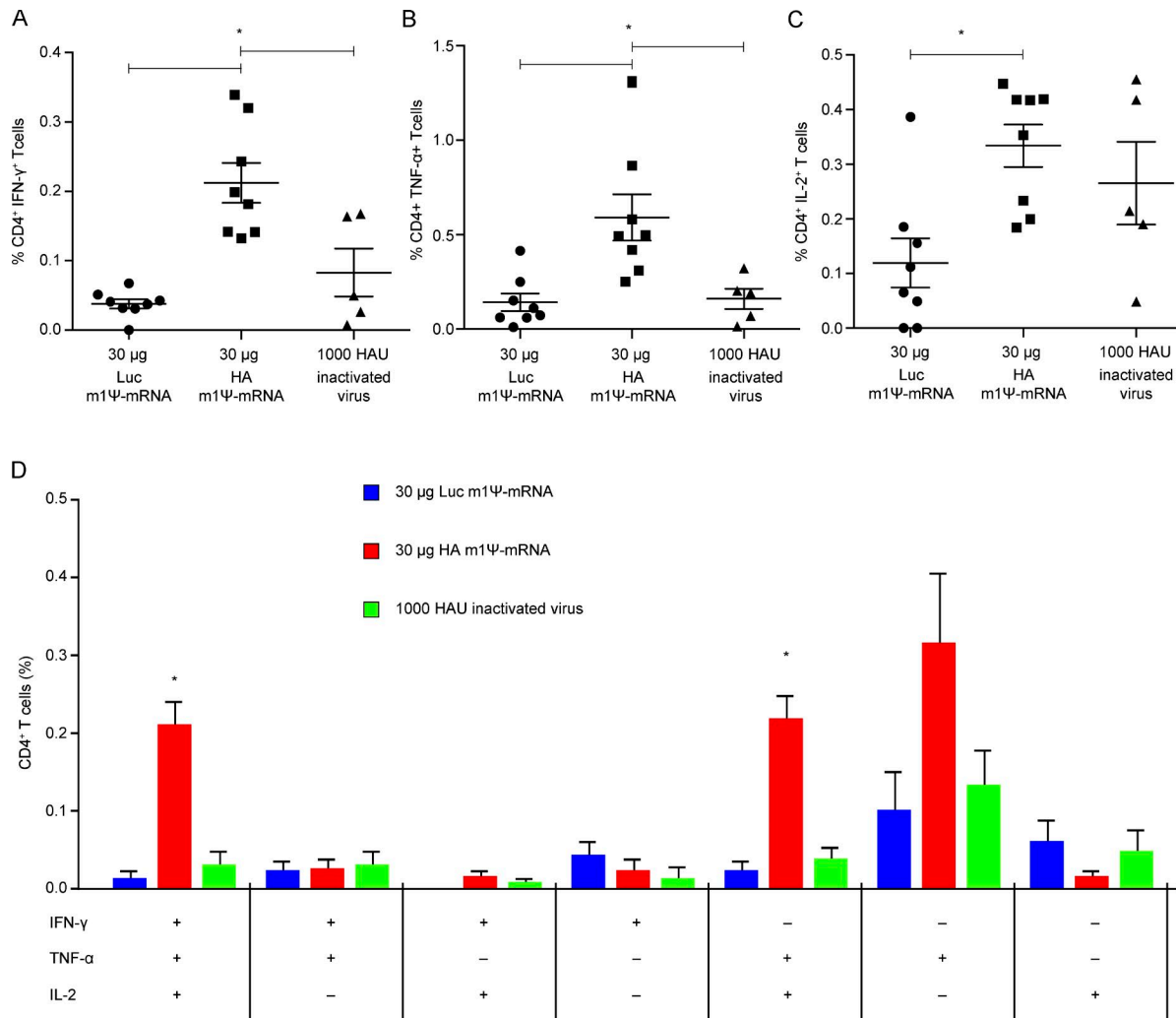
Pardi et al.
Modified mRNA vaccines induce Tfh and GC B cells

Journal of Experimental Medicine
https://doi.org/10.1084/jem.20171450

1574

Figure 3. **A single immunization with PR8 HA m1Ψ-mRNA-LNPs elicits strong antigen-specific CD4+ T cell responses.** Mice received a single i.d. injection of 30 µg of m1Ψ-mRNA-LNPs or an i.m. immunization with 1,000 hemagglutinating units (HAU) of inactivated PR8 influenza virus. Splenocytes were stimulated 10 d after immunization with HA peptides, and cytokine production by CD4+ T cells was assessed. **(A–C)** The percentages of CD4+ T cells producing IFN-γ (A), TNF-α (B), and IL-2 (C) were measured by flow cytometry. **(D)** Frequencies of combinations of cytokines produced by CD4+ T cells. n = 8–10 mice, and each symbol represents one animal. Experiments were repeated three times to achieve statistical significance. Error bars are SEM. Statistical analysis: (A–C) one-way ANOVA with Bonferroni correction, *, $P < 0.05$; (D) Student's t test, *, $P < 0.05$ compared with Luc mRNA–immunized mice.

increasing apparent affinity was observed at 8 wk (48 pM). In contrast, antibodies with much lower average, apparent affinity were detected in mice immunized with unmodified, uridine-containing mRNA or inactivated influenza viral particles (Fig. S4B). These data support a model in which increased Tfh cell responses drive a greater level of affinity maturation via somatic hypermutation; however, binding studies using purified mAbs, and sequencing of the Ig variable genes will be necessary to confirm this with certainty.

To investigate the capacity of m1Ψ-mRNA-LNPs to promote Tfh cell activity in primates, rhesus macaques (*Macaca mulatta*) were i.d. immunized with a single dose of 50 µg of clade C HIV-1 CH505 (Fera et al., 2014) Env gp160 m1Ψ-mRNA-LNPs or a single i.m. dose of 100 µg of recombinant CH505 Env gp140 protein with combined poly-inosinic and poly-cytidylic acid (poly-ICLC) adjuvant (Hiltonol, reviewed in Sultan et al., 2017). Draining lymph nodes were examined 7 d later, and total numbers of Tfh cells were enumerated by flow cytometry as CD3+CD4+CXCR5hiPD1hi cells

(Chowdhury et al., 2015). Animals immunized with m1Ψ-mRNA-LNPs exhibited substantially increased Tfh cell frequencies compared with those that received double-stranded RNA-adjuvanted Env protein immunization (Fig. 7 A and Fig. S5 A), similar to what was observed for HA in mice (Fig. 6 A). Env-specific Tfh cells were enumerated with an activation-induced marker assay (Havenar-Daughton et al., 2016). 7 d after m1Ψ-mRNA-LNP injection, 4–8% of Tfh cells were Env-specific, whereas in monkeys immunized with Env protein with poly-ICLC adjuvant, the percentage of Env-specific Tfh cells did not exceed 1% and were similar to preimmunization levels (Fig. 7 B and Fig. S5 B). The quality of antibody response in these macaques is currently under investigation.

m1Ψ-mRNA-LNP vaccination induces potent and durable neutralizing antibody responses in nonhuman primates

To evaluate the ability of the Env m1Ψ-mRNA-LNP vaccine to induce neutralizing antibody responses in nonhuman primates,
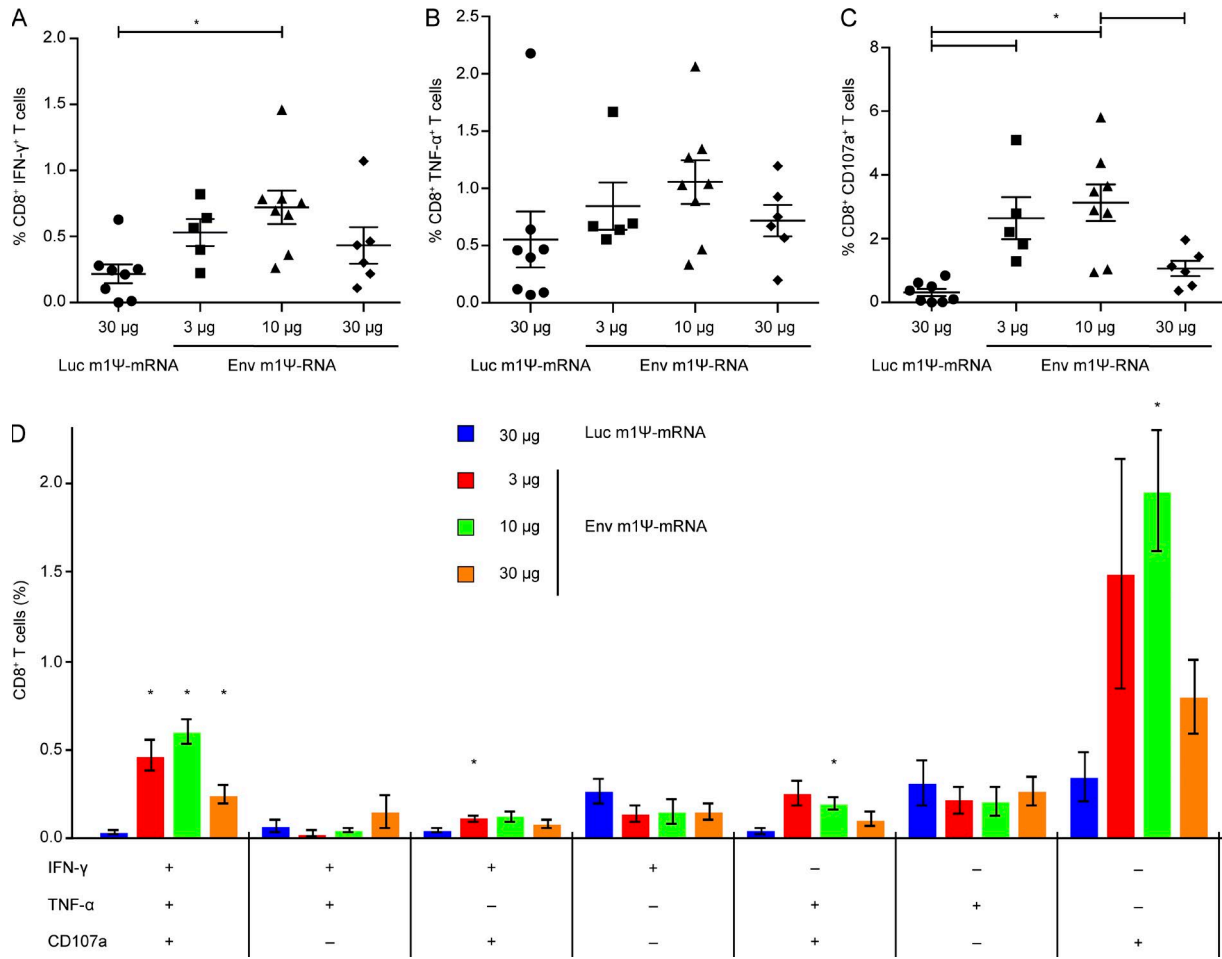
Figure 4. **Nucleoside-modified Env mRNA-LNPs elicit antigen-specific CD8+ T cell responses.** Mice received two i.d. injections of Luc or Env m1Ψ-mRNA-LNPs. **(A–C)** Percentages of CD8+ T cells producing IFN-γ (A), TNF-α (B), and CD107a (C) were analyzed. **(D)** Frequencies of combinations of cytokines and degranulation marker produced by CD8+ T cells. Splenocytes were stimulated with Env peptides, and cytokine production by CD8+ T cells was assessed by flow cytometry. n = 5–8 mice, and each symbol represents one animal. Error bars are SEM. Statistical analysis: (A–C) one-way ANOVA with Bonferroni correction, *, $P < 0.05$; (D) Student's t test, *, $P < 0.05$ compared with Luc mRNA–immunized mice.

six rhesus macaques were i.d. immunized with 50 µg of clade C HIV-1 1086C Env gp160 m1Ψ-mRNA-LNPs at weeks 0, 4, 20, and 32, and HIV-1 pseudovirus neutralization assays were performed on preimmune and wk 34 sera using the standard TZM-bl luciferase reporter system (Montefiori, 2009). Potent neutralization activity against a highly neutralization-sensitive clade C virus (MW965.26) was detected in all six animals at week 34 (Fig. 7 C, left). Importantly, three of the six animals developed neutralizing antibodies against the autologous tier 2 virus (Ce1086_B2), demonstrating the potency of the m1Ψ-mRNA-LNP vaccine platform (Fig. 7 C, right). Strikingly, one animal generated antibodies with low neutralizing activity against heterologous clade C tier 2 strains (ID_{50} values of 21 against 25710-2.43 and 31 against Ce1176_A3). Further characterization of the antibody response in these animals is under way.

To further investigate the quality and longevity of antibody responses induced by m1Ψ-mRNA-LNP immunization in rhesus macaques, a follow-up serologic analysis was conducted on animals that had been i.d. immunized with a single dose of 600 or 200 µg of ZIKV prM-E m1Ψ-mRNA-LNPs, described in a previous study (Pardi et al., 2017). Regardless of the dose, all animals

generated potent and durable neutralizing antibody responses (Fig. 7 D). Strikingly, neutralizing antibody titers were stable until the last examined time point at 12 mo after vaccination.

Nucleoside-modified mRNA-LNPs induce more potent Tfh cell, GC B cell, and plasma cell responses than unmodified mRNA-LNPs

Unmodified mRNA has been used with some success in preclinical (Schnee et al., 2016) and clinical (Alberer et al., 2017) vaccine studies, and it has been reported that unmodified mRNA can be translated at similar or higher levels in vivo compared with its nucleoside-modified counterpart, at least in the context of stringent purification (e.g., HPLC) and a sequence engineering protocol that includes a reduction in the number of uridines (Kallen et al., 2013; Thess et al., 2015). In light of these data, we sought to determine the importance of nucleoside modification in the mRNA-LNP vaccine. We therefore directly compared the magnitude of immune responses elicited by codon-optimized FPLC-purified unmodified (U) and m1Ψ-modified mRNA-LNPs. Mice were immunized with 30 µg of U- or m1Ψ-PR8 HA mRNA-LNPs by the i.d. route, and T and B cell responses were evaluated
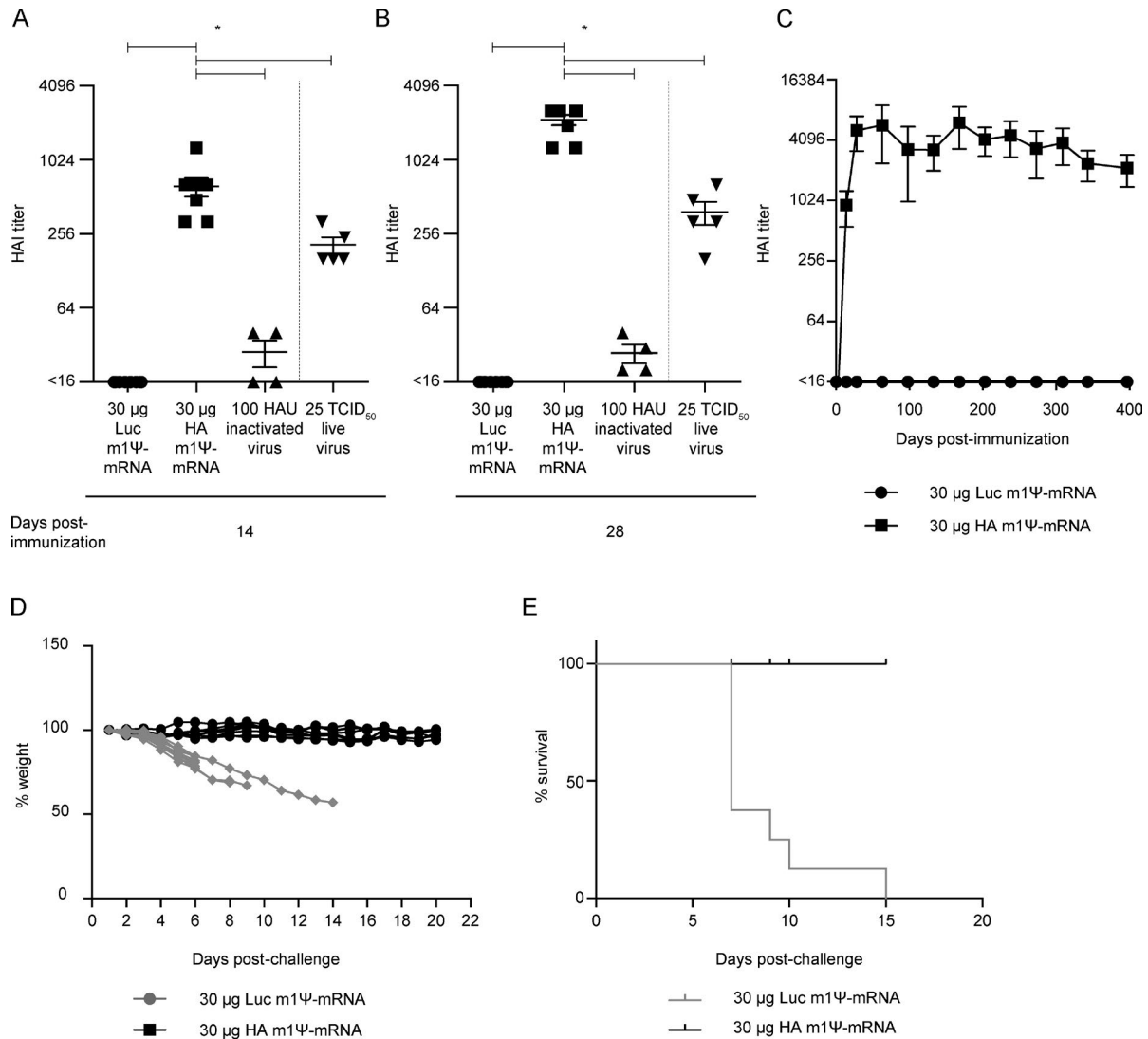
Figure 5. **HA m1Ψ-mRNA-LNP immunization elicits strong antigen-specific B cell responses.** Mice were immunized once with 30 µg of m1Ψ-mRNA-LNPs i.d. or 100 HAU of inactivated PR8 influenza virus i.m or infected with a sublethal dose (25 TCID$_{50}$) of live PR8 influenza virus. **(A–C)** HA inhibition (HAI) titers from mouse serum were determined over time. The dashed lines indicate that HAI values for the live PR8 virus infection were assayed separately. **(D and E)** Mice were challenged with a lethal dose of PR8 influenza virus 13 mo after immunization and weight loss (D) and survival (E) were followed. $n = 4–8$ mice, and each symbol represents values for one animal. Experiments were repeated at least two times. Statistical analysis: (A–B) one-way ANOVA with Bonferroni correction, *, $P < 0.05$; (C) Student's t test, comparing HA m1Ψ-mRNA with Luc m1Ψ-mRNA, *, $P < 0.05$ for each time point.

10 d after immunization. U-mRNA-LNPs induced significantly weaker CD4$^+$ T cell responses compared with m1Ψ-mRNA-LNPs (Fig. 8). Most importantly, significantly lower numbers of Tfh, GC B, and plasma cells (Fig. 9, A–D) were observed in mice that were immunized with U-mRNA-LNPs. Furthermore, U-mRNA-LNPs induced significantly lower levels of HAI activity compared with m1Ψ-mRNA-LNPs (Fig. 9 E).

mRNA-LNPs provide potent adjuvant activity for protein-subunit immunization

We hypothesized that m1Ψ-mRNA-LNPs might have adjuvant activity that favors Tfh cell, GC B cell, and neutralizing antibody development. To test that, mice were immunized i.m. with 10 µg of recombinant, purified PR8 HA protein alone or mixed with 30 µg of U-mRNA-LNPs or m1Ψ-mRNA-LNPs encoding Luc as an irrelevant protein, and immune responses were evaluated

(Fig. 10). Interestingly, addition of either unmodified or modified Luc mRNA-LNPs to PR8 HA protein resulted in slight increases in splenic Tfh cell numbers that were not statistically significant. However, the combination of PR8 HA protein with Luc m1Ψ-mRNA-LNPs resulted in a significant increase in splenic GC B cell numbers, and a lesser effect was observed with U-mRNA-LNPs (Fig. 10, A and B). Most importantly, significantly increased HAI titers were measured in animals immunized with the combined Luc U- or m1Ψ-mRNA-LNP plus PR8 HA protein vaccine compared with protein alone at 4 wk after immunization (Fig. 10 C).

Discussion

The generation of high-affinity antibodies is fundamental to neutralizing a broad range of pathogens. This work demonstrates the exceptional ability of the m1Ψ-mRNA-LNP vaccine platform
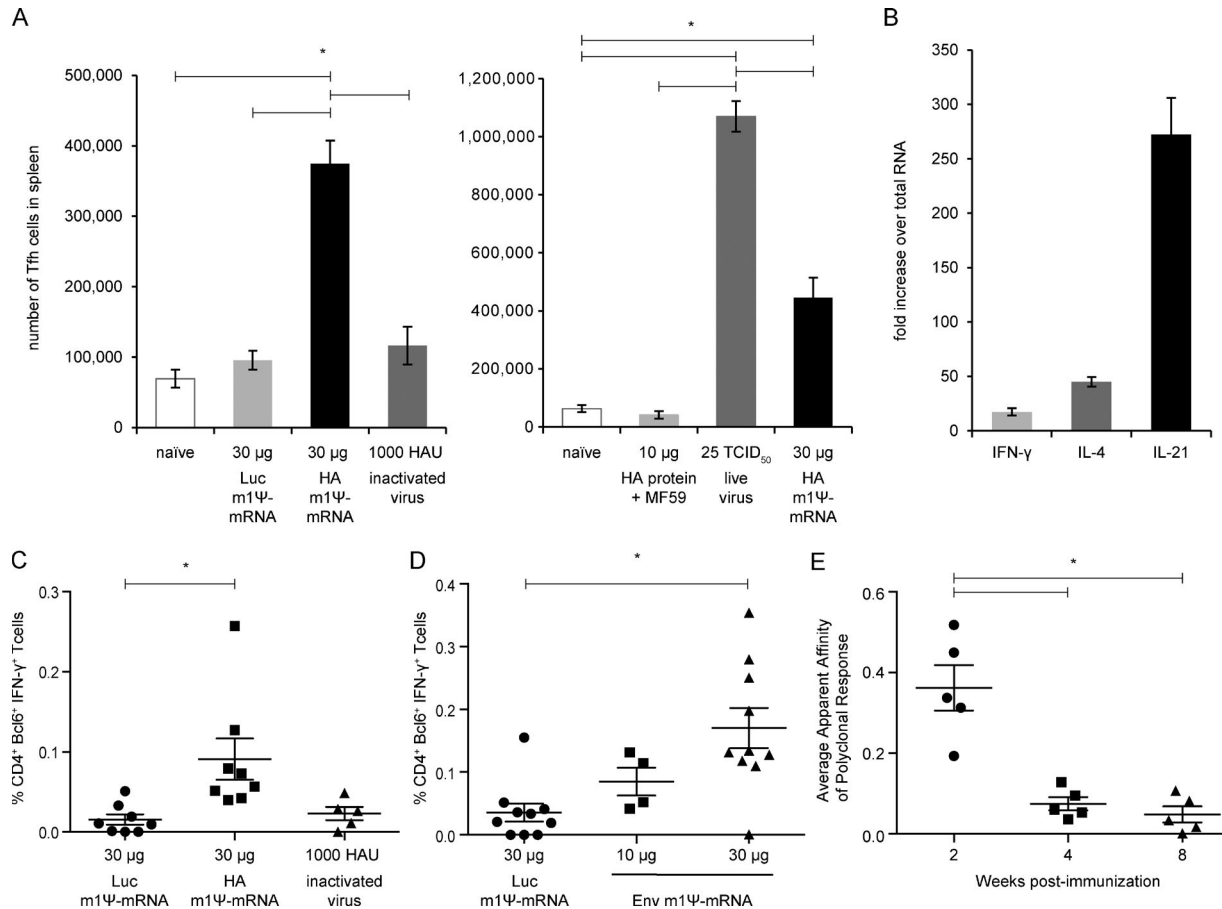
Figure 6. **Potent Tfh cell responses are elicited by a single immunization with m1Ψ-mRNA-LNPs in mice.** Mice were immunized once i.d. with 30 µg of Luc or HA m1Ψ-mRNA-LNPs, a single i.m. injection with 1,000 HAU of inactivated PR8 virus, MF59-adjuvanted recombinant PR8 HA protein, or intranasally infected with 25 $TCID_{50}$ of live PR8 influenza virus, and immune responses were examined 10 d after immunization (A and B). **(A)** Total numbers of splenic Tfh cells were determined by staining for $TCR^+CD19^-CD4^+CD62L^-CXCR5^+PD-1^+$ T cells. **(B)** IFN-γ, IL-4, and IL-21 transcript levels in sorted Tfh cells from PR8 HA m1Ψ-mRNA-LNP–immunized mice were determined by quantitative real-time RT-PCR. Fold induction of cytokines compared with total universal RNA is shown. **(C and D)** Mice were immunized with a single i.d. injection of 30 µg of HA or Env m1Ψ-mRNA-LNPs, and immune responses were examined 12 d after immunization. Percentage of IFN-γ producing $CD4^+Bcl-6^+$ Tfh-like cells was measured by flow cytometry after HA (C) or Env (D) peptide stimulation. **(E)** Mice were immunized with a single i.d. injection of 30 µg of PR8 HA m1Ψ-mRNA-LNPs, and rates of binding to PR8 HA were examined 2, 4, and 8 wk later by biolayer interferometry. The apparent nanomolar affinity of anti–HA antibodies, derived from the mean rates of HA-binding in polyclonal sera, is plotted for each serum sample, with lower values corresponding to higher apparent affinity. n = 5–8 mice, and each symbol represents values for one animal. Experiments were repeated at least two times to achieve sufficient numbers of values for mice in each group. Error bars are SEM. Statistical analysis: one-way ANOVA with Bonferroni correction, *, $P < 0.05$.

to generate high levels of neutralizing antibodies against influenza virus, ZIKV, and HIV-1. A single immunization with HA m1Ψ-mRNA-LNPs generated class-switched, protective antibody responses by 10–14 d after immunization (Figs. 5 and 9 E). Influenza HAI titers increased for 8 wk after immunization, which is indicative of potent GC reactions. A direct correlate of this GC reaction is that HAI titers induced by a single immunization with HA m1Ψ-mRNA-LNPs were ∼40-fold greater than those induced by an inactivated viral particle vaccine (Fig. 5, A and B), and remarkably, they were approximately four times greater than those induced by pathogenic infection (Fig. 5, A and B). Importantly, these high HAI titers were maintained for at least 13 mo (Fig. 5 C). Because relatively weak $CD8^+$ T cell responses were measured after a single immunization with HA m1Ψ-mRNA-LNPs (unpublished data), it is likely that the potent, neutralizing, anti-HA antibodies played a critical role in protecting these mice

from lethal PR8 influenza virus challenge 13 mo after a single immunization (Fig. 5, D and E).

Tfh cell responses have been identified as a critical need for an effective and durable HIV vaccine (Havenar-Daughton et al., 2017). High numbers of activated Tfh cells have been associated with the development of neutralizing antibody breadth in non-human primates infected with a chimeric simian/human immunodeficiency virus (Yamamoto et al., 2015). Broadly neutralizing antibodies isolated from HIV-infected individuals show an unusually high degree of somatic diversification (Kwong and Mascola, 2012), a process that is driven by Tfh cells. In addition, many HIV-1 vaccine studies, including the RV144 vaccine trial, have observed poor durability of Env-specific neutralizing antibody responses in humans, along with the inability to develop tier 2 neutralization activity (Montefiori et al., 2012), which may be related to insufficient Tfh cell responses. In this study, we
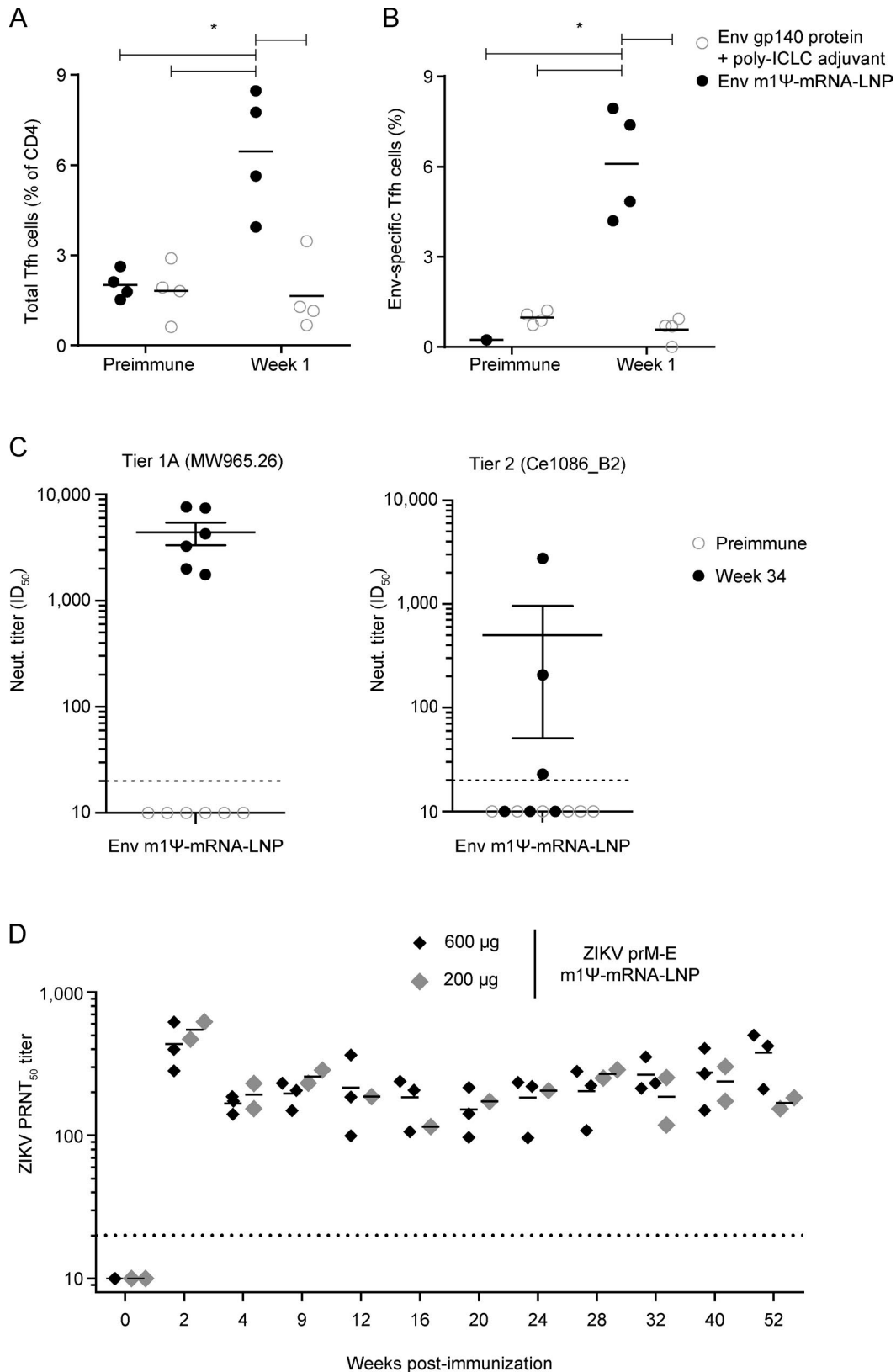
Figure 7. **Potent Tfh cell and sustained neutralizing antibody responses are elicited by a single immunization with m1Ψ-mRNA-LNPs in nonhuman primates. (A and B)** Rhesus macaques were immunized with 50 µg of CH505 Env m1Ψ-mRNA-LNPs or 100 µg of Env gp140 protein + poly-ICLC adjuvant, and Tfh cell responses in draining lymph nodes were analyzed 7 d after immunization. (A) The percentage of Tfh cells (CXCR5^{hi}PD1^{hi}) among total CD4$^+$ T cells in lymph nodes is shown. (B) Lymph node cells were analyzed for Env-specific Tfh cells by activation-induced marker assay. The percentage of OX40$^+$CD25$^+$ cells in the Tfh gate (CD4$^+$CXCR5^{hi}PD1^{hi} cells) after stimulation with Env peptide pool + protein is shown. The percentage of Env-specific Tfh cells for each sample was calculated as the percentage of OX40$^+$CD25$^+$ in Env-stimulated conditions minus the percentage of OX40$^+$CD25$^+$ in unstimulated conditions. Each point represents one

provide evidence that HIV-1 Env m1Ψ-mRNA-LNP immunization elicited detectable neutralizing antibodies against the autologous tier 2 virus in rhesus macaques (Fig. 7 C). Further characterization of neutralizing antibody quality and durability in this nonhuman primate study is under way. A recent study from our laboratory, targeting ZIKV, also demonstrated that m1Ψ-mRNA-LNP vaccination was an effective vaccine strategy in nonhuman primates (Pardi et al., 2017). A single dose of ZIKV prM-E m1Ψ-mRNA-LNP vaccine induced potent neutralizing antibodies that protected animals from a live virus challenge (Pardi et al., 2017). Here, we show that these antibodies persisted long-term (≥12 mo), with no decrease in titer (Fig. 7 D).

To determine the basis of this potent and durable neutralizing antibody response, we characterized the GC B cell and Tfh cell responses in the secondary lymphoid tissues of immunized animals and found that both cell types were robustly elicited by a single immunization with the m1Ψ-mRNA-LNP platform. This contrasted markedly with the inactivated virus and adjuvanted protein vaccines (Figs. 6, 7, and 9 and Fig. S3). These results demonstrate that the magnitude of the Tfh and GC B cell responses may be a critical factor driving the efficacy of the m1Ψ-mRNA-LNP platform compared with other vaccine approaches. Additionally, the potency of Tfh cell induction by the m1Ψ-mRNA-LNP vaccine in nonhuman primates (Fig. 7, A and B) suggests potential applicability to humans. Our findings in nonhuman primates were corroborated by a recent study that reported the presence of circulating Tfh-like cells in rhesus macaques after two immunizations with an influenza HA m1Ψ-mRNA-LNP vaccine that was prepared similarly, except that the mRNA was not FPLC-purified (Lindgren et al., 2017). The present study extends this line of analysis by characterizing bona fide lymphoid organ Tfh and GC responses to several antigens in two animal species, with comparisons to multiple other vaccine formats. In addition, our results suggest that both the LNP component and the m1Ψ modified nucleoside in the mRNA contribute to the striking potency of these and other published m1Ψ-mRNA-LNP vaccines (Bahl et al., 2017; Liang et al., 2017; Pardi et al., 2017).

Because Tfh cells are critical for inducing long-lived neutralizing antibodies, considerable effort has gone into the development of vaccines and adjuvants that promote Tfh cell responses. However, the literature is currently divided on the requirements for Tfh cell generation. A number of reports have found that certain adjuvant activities are required for potent Tfh cell induction (Cucak et al., 2009; Wang et al., 2014; Mastelic Gavillet et al., 2015; Riteau et al., 2016), whereas others have reported that proinflammatory signals are unnecessary or even detrimental to strong Tfh cell responses (Lahoud et al., 2011; Chen et al., 2013; Kato et al., 2015; Yao et al., 2015; Locci et al., 2016). Two recent studies have demonstrated that extended antigen availability is a strong driver of GC reactions and potent Tfh cell and

neutralizing antibody responses (Tam et al., 2016; Pauthner et al., 2017). In this study, we confirmed our previous finding (Pardi et al., 2015) that i.d. injection with m1Ψ-mRNA-LNPs resulted in sustained protein production in vivo (Fig. 1). In contrast, unmodified U-mRNA-LNPs were translated at significantly lower levels and for shorter durations (Fig. 1, D–F), and they were associated with significantly weaker immune responses (Figs. 8 and 9). As no established adjuvant was included in the m1Ψ-mRNA-LNP vaccines, we hypothesized that the mRNA-LNPs themselves might have an adjuvant activity that also contributed to potent Tfh cell and GC B cell activation. To examine this possibility, mice were immunized with recombinant PR8 HA protein alone or in combination with either Luc U-mRNA-LNPs or Luc m1Ψ-mRNA-LNPs. Addition of Luc m1Ψ-mRNA-LNPs, or, to a lesser extent, U-mRNA-LNPs, to the PR8 HA protein subunit vaccine resulted in massive increases in splenic GC B cell numbers compared with PR8 HA protein alone, revealing that mRNA-LNPs do exert an adjuvant effect in this context. Interestingly, no significant differences in splenic Tfh cell numbers were noted between these immunogen groups, suggesting the possibility that the adjuvant activity of mRNA-LNPs may be exerted specifically on GC B cells and that, perhaps, Tfh cells are activated indirectly as a consequence. Indeed, multiple studies have provided evidence about the dynamic interaction and interdependence of these two cell types (Victora and Nussenzweig, 2012; Crotty, 2014). However, further investigation is needed to understand how GC B cell responses are enhanced by an mRNA-LNP adjuvant, despite similar Tfh cell responses. Although both formats of mRNA-LNP adjuvant did not increase Tfh cell numbers in the context of HA protein immunization, the HA-encoding mRNA-LNPs did increase Tfh cells over other vaccine formats, and that effect was dependent on the modified nucleoside (Figs. 6 and 9). Taken together, our mechanistic data—in accordance with the literature—suggest that there are at least two likely contributors to the potent GC B cell, Tfh cell, and neutralizing antibody responses generated by the m1Ψ-mRNA-LNP vaccine platform: first, robust and sustained antigen production from the nucleoside-modified mRNA-LNP vector, and second, adjuvant effects of the mRNA-LNP vaccine that favor GC B cell activation. Future studies will provide details about the exact cell-signaling pathways involved in these processes and whether nucleoside modification also contributes to Tfh and GC B cell activation by an immunogen dose-independent mechanism.

Here, we provide a body of evidence that the m1Ψ-mRNA-LNP vaccine platform induces strong Tfh and GC B cell immune responses, which generate high levels of long-lived neutralizing antibodies in mice and rhesus macaques. This vaccine platform has the additional advantages of a favorable safety profile, potentially inexpensive manufacturing, and the capacity for rapid development in emerging epidemics. Production of mRNA-based vaccines is amenable to large-scale and

---

animal. **(C)** Rhesus monkeys were immunized with 50 µg of 1086C Env m1Ψ-mRNA-LNPs at weeks 0, 4, 20, and 32, and neutralization titers (expressed as the reciprocal serum dilution resulting in ID_{50}) from preimmune and week 34 sera were determined against the MW965.26 (tier 1A) and autologous Ce1086_B2 (tier 2) viruses. Each point represents one animal. **(D)** Rhesus macaques were immunized with 600 µg ($n = 4$) or 200 µg ($n = 3$) of ZIKV prM-E m1Ψ-mRNA-LNPs, and the antibody response was measured by PRNT against ZIKV MR-766. Points represent individual monkeys; horizontal lines indicate the mean. Statistical analysis: (A–B) two-way ANOVA with Bonferroni correction, *, $P < 0.05$; (D) dose groups were compared by Kruskal-Wallis test, *, $P > 0.05$ for all comparisons.
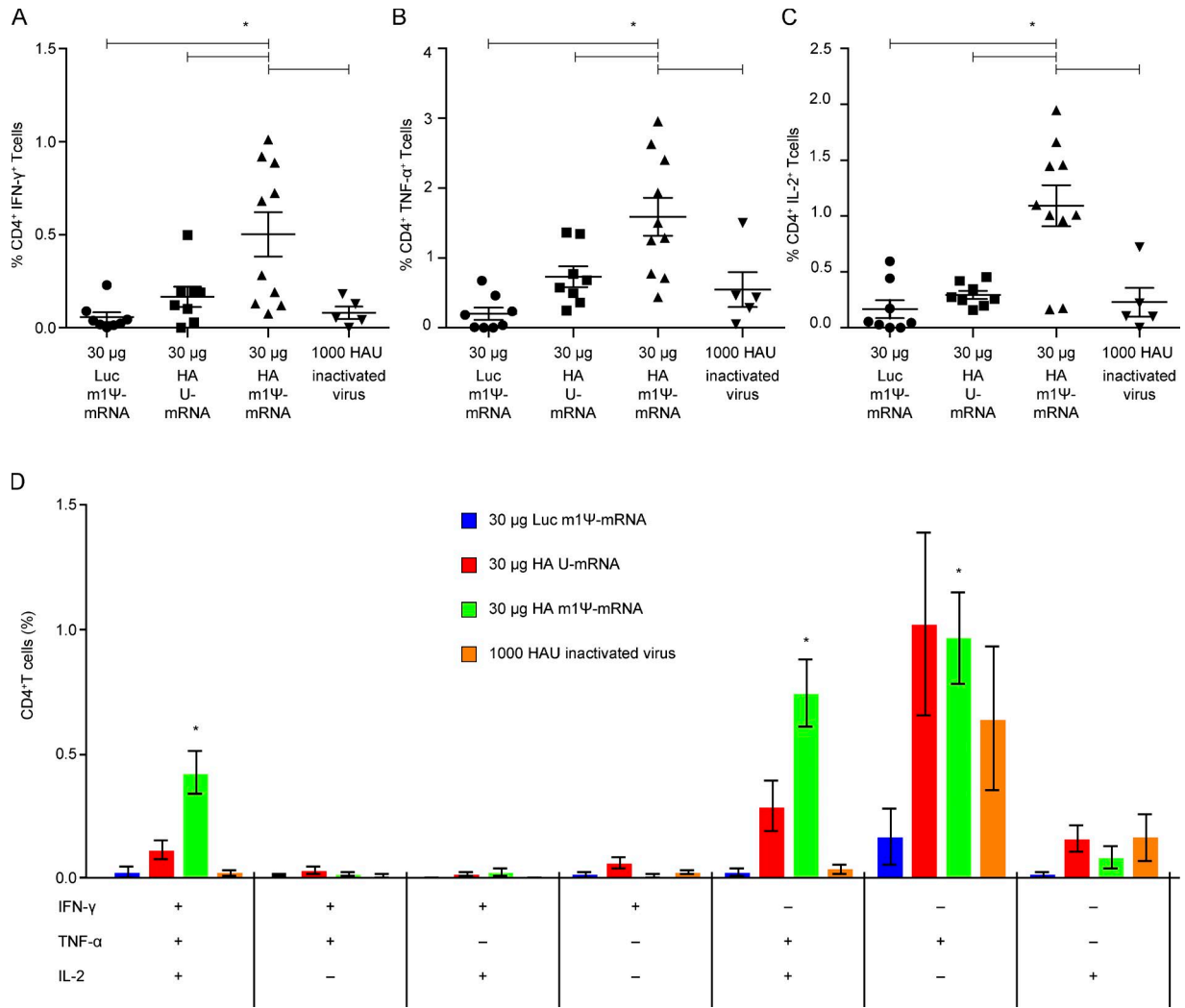
Figure 8. **Nucleoside modification induces superior CD4+ T cell responses compared with unmodified mRNA.** Mice received a single i.d. injection of 30 µg of Luc m1Ψ-mRNA-LNPs, HA U-mRNA-LNPs, HA m1Ψ-mRNA-LNPs or an i.m. immunization with 1,000 HAU of inactivated PR8 influenza virus. Splenocytes were stimulated 10 d after immunization with HA peptides and cytokine production by CD4+ T cells was assessed. **(A–C)** The percentage of CD4+ T cells producing IFN-γ (A), TNF-α (B), and IL-2 (C) was measured by flow cytometry. **(D)** Frequencies of combinations of cytokines produced by CD4+ T cells. n = 5–10 mice, and each symbol represents one animal. Experiments were repeated at least two times to achieve statistical significance. Error bars are SEM. Statistical analysis: (A–C) one-way ANOVA with Bonferroni correction, *, $P < 0.05$; (D) Student's t test, *, $P < 0.05$ compared with Luc mRNA–immunized mice.

economical manufacturing because of the high yield of in vitro transcription reactions. The generation of mRNA is sequence independent and, thus, highly versatile, and both the mRNA and LNP components are in Current Good Manufacturing Practice production. The combined characteristics of m1Ψ-mRNA-LNPs render it a valuable vaccine platform for many applications, including emerging viral diseases, neglected tropical diseases, and pathogens for which current vaccines are inadequate.

Materials and methods
Ethics statement
The investigators faithfully adhered to the *Guide for the Care and Use of Laboratory Animals* by the Committee on Care of Laboratory Animal Resources Commission on Life Sciences, National Research Council.

Mice
The animal facilities at the University of Pennsylvania and The Wistar Institute of Anatomy and Biology vivarium are fully accredited by the American Association for Assessment and Accreditation of Laboratory Animal Care. All studies were conducted under protocols approved by the University of Pennsylvania and The Wistar Institute of Anatomy and Biology institutional animal care and use committees.

Monkeys
Rhesus macaques (*Macaca mulatta*) of Indian origin were housed in American Association for Assessment and Accreditation of Laboratory Animal Care–accredited facilities, and all procedures were conducted with Duke University, University of Pennsylvania, University of Washington, and Bioqual institutional animal care and use committee approval.
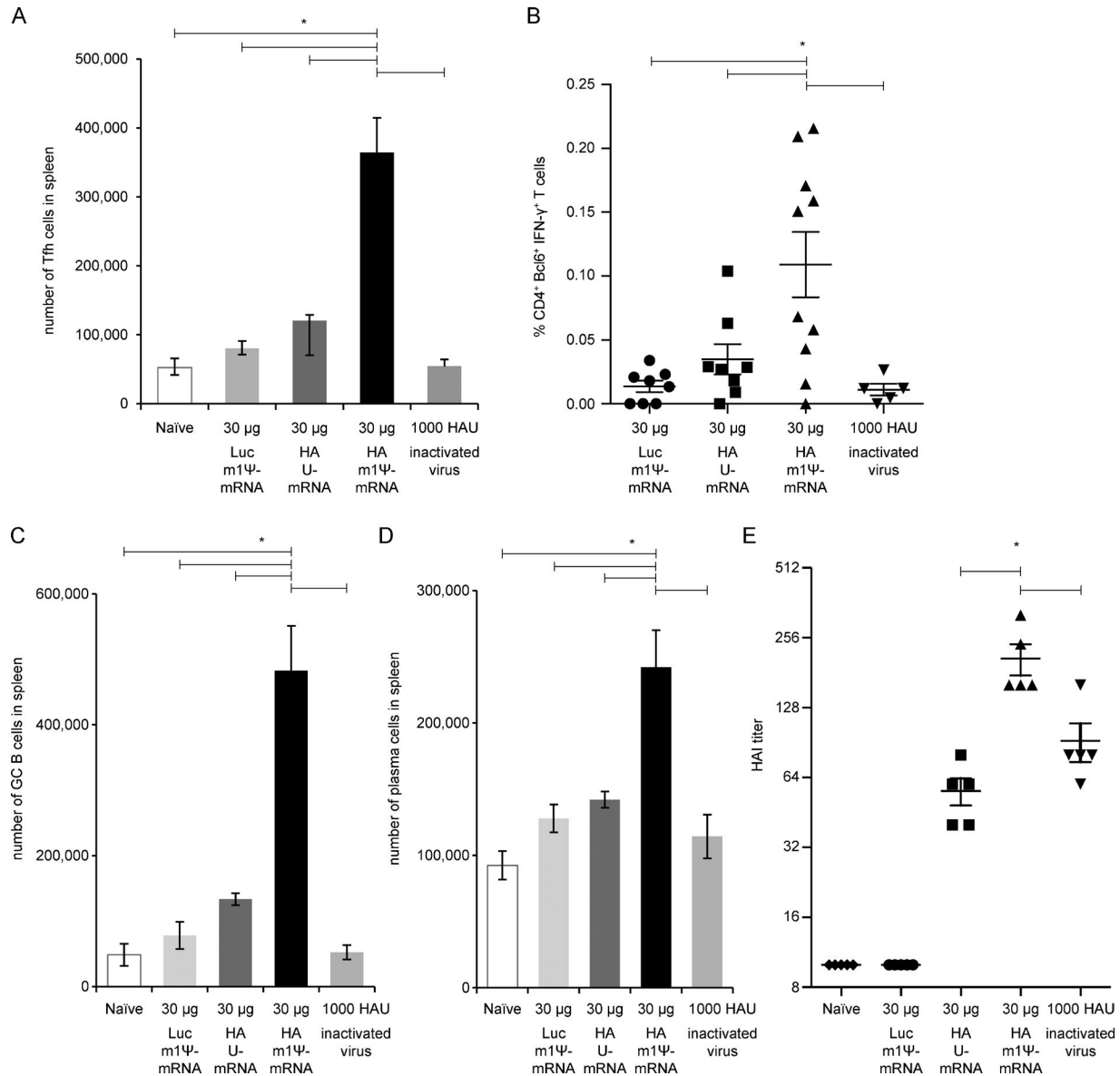
Figure 9. **A single immunization with m1Ψ HA mRNA-LNPs induces more potent Tfh cell responses, higher splenic GC B and plasma cell numbers, and higher HAI titers compared with unmodified mRNA-LNPs.** Mice were immunized with a single i.d. injection of 30 μg of Luc m1Ψ-mRNA-LNP, HA U- or m1Ψ-mRNA-LNPs, or a single i.m. immunization of 1,000 HAU of inactivated PR8 virus, and immune responses were examined 10 d later. **(A)** The total number of splenic Tfh cells was counted by staining for TCRβ⁺CD19⁻CD4⁺CD62L⁻CXCR5⁺PD-1⁺ T cells. **(B)** Percentage of IFN-γ producing CD4⁺Bcl6⁺ Tfh-like cells was measured by flow cytometry. **(C and D)** Total numbers of splenic GC B cells (C) and plasma cells (D) were determined. **(E)** HAI titers from mouse serum were determined 10 d after immunization. n = 5–10 mice, and each symbol represents values for one animal. Experiments were repeated at least two times to achieve statistical significance. Error bars are SEM. Statistical analysis: one-way ANOVA with Bonferroni correction, *, $P < 0.05$.

mRNA production

mRNAs were produced as described previously (Pardi et al., 2013) using T7 RNA polymerase (Megascript; Ambion) on linearized plasmids encoding codon-optimized (Thess et al., 2015) Luc (pTEV-new Luc2-A101), a variant of R3A (dual-tropic, clade B) gp160 HIV-1 Env (Meissner et al., 2004), which was adapted to a CD4⁻ SupT1-derived cell line (pTEV-iR3A Env-A101), HIV-1 CH505 gp160 Env (pTEV-CH505 trimer-A101), HIV-1 1086C gp160 Env (pTEV-1086C Env-A101), PR8 influenza virus HA (pTEV-PR8 HA-A101), and ZIKV prM-E (pTEV-ZIKVprM-E-A101) from the strain H/PF/2013 (Asian lineage, French Polynesia,

2013, GenBank accession no. KJ776791). The iR3A sequence was provided by J.A. Hoxie (University of Pennsylvania, Philadelphia, PA). mRNAs were transcribed to contain 101 nucleotide-long poly(A) tails. m1Ψ-5′-triphosphate (TriLink BioTechnologies), instead of uridine triphosphate, was used to generate modified nucleoside-containing mRNA. RNAs were capped using the m7G capping kit with 2′-O-methyltransferase (ScriptCap; CellScript) to obtain cap1 mRNA was purified by FPLC (Akta Purifier; GE Healthcare Life Sciences), as described previously (Weissman et al., 2013). All mRNAs were analyzed by denaturing or native agarose gel electrophoresis and were stored frozen at –20°C.
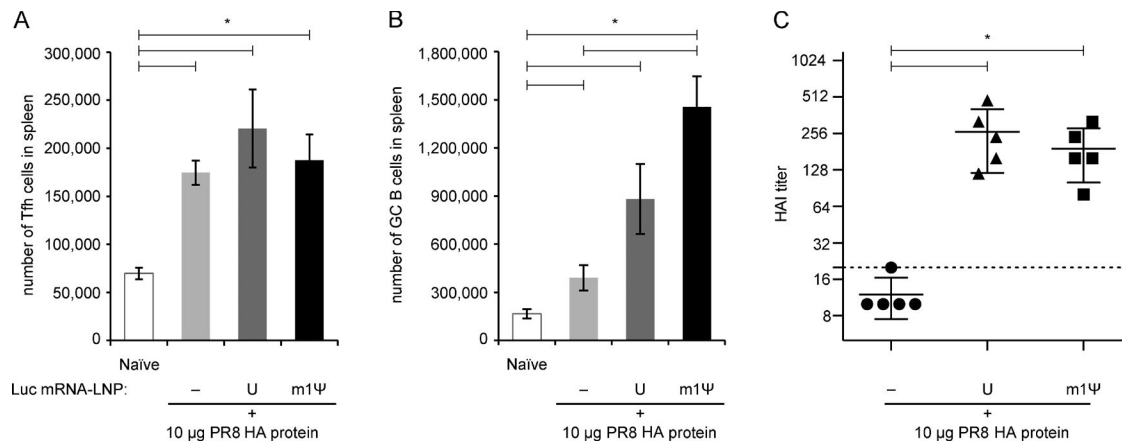
Figure 10. **mRNA-LNPs provide potent adjuvant activity in a protein subunit vaccine.** Mice were immunized with a single i.m. injection of 10 μg of recombinant PR8 HA protein alone or in combination with 30 μg of Luc U- or m1Ψ-mRNA-LNPs. **(A and B)** Total number of splenic Tfh cells (A) and GC B cells (B) were determined 12 d after immunization. **(C)** HAI titers were measured 4 wk after immunization. Error bars are SEM. n = 5 mice. Statistical analysis: one-way ANOVA with Bonferroni correction, *, $P < 0.05$.

LNP formulation of the mRNA

FPLC-purified, m1Ψ-containing Luc; HIV-1 Env; ZIKV prM-E; and influenza virus HA-encoding mRNAs were encapsulated in LNPs, using a self-assembly process in which an aqueous solution of mRNA at 4.0 pH is rapidly mixed with a solution of lipids dissolved in ethanol (Maier et al., 2013). LNPs used in this study were similar in composition to those described previously (Jayaraman et al., 2012; Maier et al., 2013) and contained an ionizable cationic lipid (proprietary to Acuitas Therapeutics)/phosphatidylcholine/cholesterol/polyethylene glycol/lipid (50:10:38.5:1.5 mol/mol) encapsulated at an RNA to total lipid ratio of ~0.05 (wt/wt). The LNPs had a diameter of ~80 nm, as measured by dynamic light scattering using a Zetasizer Nano ZS instrument (Malvern Instruments). mRNA-LNP formulations were stored at –80°C at an mRNA concentration of ~1 μg/μl.

Immunization of mice and monkeys
Mice
Female BALB/c mice aged 8 wk were purchased from Charles River Laboratories. mRNA-LNPs were diluted in sterile PBS and injected into animals i.d. with a 3/10-cc, 29 1/2-gauge insulin syringe (BD Biosciences). Four sites of injection (30 μl each) over the lower back were used. Inactivated PR8 influenza virus stock was diluted to 100 or 1,000 HAUs per 30 μl and injected into the quadriceps muscle with a 3/10-cc, 29 1/2-gauge insulin syringe. Similarly, PR8 HA recombinant protein was diluted in sterile PBS and administered in a 30 μl volume, i.m. For MF59-adjuvanted PR8 HA recombinant protein vaccination, PR8 HA recombinant protein was diluted in sterile PBS to 15 μl and mixed with 15 μl of MF59 before i.m. administration. For live virus infection studies, animals were intranasally inoculated with 25 TCID$_{50}$ of PR8 influenza virus under isoflurane anesthesia.

Monkeys
Ketamine anesthetized animals were shaved on their back and injected i.d. with mRNA-LNPs diluted in PBS. Ten sites of injection (60 μl each) were used. Animals of similar age and weight were randomly designated to dose groups. For i.m. injections, 100 μg of soluble CH505 gp140, formulated with 1 mg poly-ICLC (Hiltonol, Oncovir) was injected in one quadriceps (Martins et al., 2014). 7 d after vaccination, an inguinal lymph node was obtained.

Blood collection
Mice
Blood was collected before each immunization from the orbital sinus under isoflurane anesthesia or by submandibular bleeding and, at the end of the vaccination studies, by cardiac puncture during euthanasia. Blood was centrifuged for 10 min at 3,000 revolutions per minute (rpm) in an Eppendorf microcentrifuge, and the serum was stored at –80°C and used for ELISA and virus-neutralization assays.

Monkeys
Blood was collected by femoral or peripheral venipuncture under ketamine anesthesia. Serum separator tubes were centrifuged for 20 min at 1,750 rpm, and serum was collected and stored at –80°C for ELISA and neutralization analysis.

Influenza virus challenge studies
Mice were challenged intranasally with 5,000 TCID$_{50}$ of A/Puerto Rico/8/1934 influenza virus.

Antibody reagents
The following antibodies were used for flow cytometry: anti–CD4 PerCP/Cy5.5 (clone GK1.5; BioLegend), anti–CD4 AF700 (clone OKT4; BioLegend), anti–CD8a PB (clone 53-6.7; BioLegend), anti–CXCR5 BV605 (clone L138D7; BioLegend), anti–CXCR5-biotin (clone MU5UBEE; eBioscience), anti–CXCR5 PE-Cy7 (streptavidin; BD Biosciences), anti–PD-1 BV785 (clone 29F.1A12; BioLegend), anti–PD-1 BV421 (clone EH12.2H7; BioLegend), anti–OX40 PE (clone L106; BD Biosciences), anti–CD25 BV650 (clone BC96; BioLegend), anti–Bcl6 PE (clone K112-91; BD Biosciences), anti–ICOS BV421 (clone 7E.17G9; BD Biosciences), anti–CD27 PE (clone LG.3A10; BD Biosciences), anti–CD107a FITC (clone 1D4B; BD Biosciences), anti–CD3 allophycocyanin (APC)-Cy7 (clone 145-2C11;

BD Biosciences), anti–CD3 APC-Cy7 (clone SP34-2; BD Biosciences), anti–TNF-α PE-Cy7 (clone MP6-XT22; BD Biosciences), anti–IFN-γ AF700 (clone XMG1.2; BD Biosciences), anti–IL-2 APC (clone JES6-5H4; BD Biosciences), and anti–Foxp3 APC (clone PCH101; eBioscience).

The following antibodies were used for cell sorting: anti-CD4 PE–Texas red (clone RM4-5; BioLegend), anti–CXCR5 PE (clone L138D7; BioLegend), anti–PD-1 PE-Cy7 (clone RMP1-30; BioLegend), anti–IgM PE-CF594 (clone R6-60.2; BD Biosciences), anti–IgM APC (clone II/41; BD Biosciences), anti–IgD BV421 (clone 11-26c.2a; BioLegend), anti–CD38 AF700 (clone 90; eBioscience), anti–CD138 BV605 (clone 281–2; BioLegend), anti–B220 AF647 (clone RA3-6B2; BioLegend), anti–CD62L AF700 (clone MEL-14; eBioscience), anti–TCR-β BV421 (clone H57-597; BioLegend), anti–F4/80 PE-Cy5 (clone BM8; eBioscience), anti–CD19 APC Cy7 and BV785 (clone 6D5; BioLegend), anti–Ly-6G/GR1 PE-Cy5 (RB6-8C5; eBioscience), and PNA-FITC (Sigma). LIVE/DEAD Fixable Aqua Dead Cell Stain Kit (Life Technologies) or Zombie L/D Aqua (BioLegend) was used to discriminate dead cells and debris.

The following antibodies were used for ELISA assays: goat anti–mouse IgG horseradish peroxidase conjugate (Sigma) was used as a detection antibody for measuring anti–gp120. 3B3 anti–HIV-1 gp120 mAb (12560; AIDS Reagent Program, National Institutes of Health [NIH]; Gao et al., 2009) was used to generate a standard curve.

Peptides, proteins, and adjuvants

The following reagent was obtained through the NIH AIDS Reagent Program: HIV-1 subtype B (MN) and Env peptide set. BEI Resources provided the HA PR8 influenza peptide array (NR-18973). The coating antigen for ELISA assays was an HIV-1 gp120 from the HXBc2 isolate, which was prepared as described previously (Guo et al., 2013). The blocking protein for ELISA assays was BSA (Sigma). The recombinant PR8 HA protein was purchased from Sino Biological Inc. (catalog number 11684-V08H) and was reconstituted in sterile PBS. The MF59 adjuvant (AddaVax) was purchased from InvivoGen.

ELISA

HIV-1 gp120-specific IgG in mouse serum was measured by ELISA. Immulon 4 HBX high-binding plates were coated with 100 µl of purified HIV-1 HXBc2 gp120 at a final concentration of 1 µg/ml in PBS overnight at 4°C. The plates were washed once with wash buffer (0.05% Tween-20 in PBS) and then blocked with blocking buffer (2% BSA in PBS) for 1 h at room temperature; after which, the plates were washed three times with wash buffer. Dilutions of serum samples and standard for the gp120-specific IgG measurement (mouse mAb against gp120 [3B3]) were made in blocking buffer and incubated on the plate (100 µl/well) for 1.5 h at room temperature. Samples and standard were removed, and the plate was washed four times with wash buffer. Detection antibody was diluted 1:10,000 in blocking buffer and incubated (100 µl/well) for 1 h. After four washes, TMB substrate mixture (KPL) was added at 100 µl/well for 20 min; 2 N sulfuric acid (50 µl/well) was used to stop the reaction, and the optical density was read at 450 nm on a Dynex MRX Revelation microplate reader. The linear region of the standard curve was used for quantitation.

HIV-1 virus neutralization assays

Neutralizing antibody activity was measured in 96-well culture plates by Tat-regulated Luc reporter gene expression to quantify reductions in virus infection in TZM-bl cells. TZM-bl cells were obtained from the NIH AIDS Reagent Program, as contributed by J. Kappes and X. Wu. Assays were performed with HIV-1 Env-pseudotyped viruses, as described previously (Montefiori, 2009). Test samples were diluted over a range of 1:20 to 1:43,740 in cell culture medium and preincubated with virus (~150,000 relative light unit equivalents) for 1 h at 37°C before addition of cells. After a 48-h incubation, cells were lysed, and Luc activity was determined with a microtiter plate luminometer and BriteLite Plus Reagent (Perkin Elmer). Neutralization titers are the serum dilution at which relative luminescence units (RLUs) were reduced by 50% compared with RLUs in virus control wells after subtraction of background RLUs in cell control wells. Serum samples were heat-inactivated at 56°C for 1 h before assay.

The virus neutralization activity of immune sera was measured against HIV-1 strains MW965.26, Ce1086_B2, 25710-2.43, and Ce1176_A3.

HAI assays

Sera were heat treated for 30 min at 55°C. Titrations were performed in 96-well, round-bottom plates (BD Biosciences). Sera were serially diluted twofold and added to four agglutinating doses of virus in a total volume of 100 µl. Turkey erythrocytes (Lampire Biological Laboratories) were added (12.5 µl of a 2% [vol/vol] solution). The erythrocytes were gently mixed with sera and virus, and agglutination was read after incubating for 1 h at room temperature. HAI titers were expressed as the inverse of the highest dilution that inhibited four agglutinating doses of influenza virus.

Plaque reduction neutralization tests (PRNTs)

ZIKV strain MR-766 (African lineage, Uganda, 1947, GenBank accession no. AY632535; University of Texas Medical Branch Arbovirus Reference Collection) was produced in Vero cells (CCL-81; ATCC), and 50 plaque-forming units were incubated with increasing dilutions of heat-inactivated macaque sera in serum-free DMEM (Corning) for 1 h at 37°C. The virus/serum mixture (200 µl) was added to a confluent monolayer of Vero cells in a 6-well format and incubated for 1.5 h at 37°C with intermittent rocking. Then, 3 ml of overlay, containing a final concentration of 0.5% methylcellulose (4,000 centipoise; Sigma), 1× DMEM (Gibco), 16 mM Hepes, 0.56% sodium bicarbonate, 1.6× GlutaMAX (Gibco), 1× penicillin/streptomycin (Corning), and 4 µg/ml amphotericin B (Gibco), was added to each well, and plates were incubated for 5 d at 37°C in 5% CO_2. The overlay was aspirated, and cells were fixed and stained with 0.5% crystal violet (Sigma) in 25% methanol with 75% deionized water. Wells were rinsed with deionized water to visualize plaques. Neutralization titers ($PRNT_{50}$) were determined by plotting a line through the linear portion of the curve that crossed 50% inhibition and calculating the reciprocal dilution of sera required for 50% neutralization of infection. $PRNT_{50}$ titers below the limit of detection are reported as half of the limit of detection.

Stimulation and staining of cells
Mice
Spleen single-cell suspensions were made in complete medium. Splenocytes were washed once in PBS and resuspended in complete medium at 2×10^7 cells/ml. 2×10^6 cells (100 µl) per sample were stimulated for 6 h at 37°C using four overlapping HIV-1 Envs (MN) or two influenza HA (A/Puerto Rico/8/34) peptide pools at 2 µg/ml per peptide. Golgi Plug (brefeldin A; BD Biosciences) and Golgi Stop (monensin; BD Biosciences) were diluted 1:100 and 1:143 in complete medium, respectively, and 20 µl from each was added to each sample to inhibit the secretion of intracellular cytokines after 1 h of stimulation. A phorbol 12–myristate-13–acetate (PMA; 10 ng/ml)–ionomycin (250 ng/ml; Sigma)–stimulated sample and unstimulated samples for each animal were included.

After stimulation, cells were washed in PBS and stained with the LIVE/DEAD Fixable Aqua Dead Cell Stain Kit and then surface stained for CD4, CD8, and CD27 in the T helper 1 (Th1) panel and CD4, CXCR5, and PD-1 in the Tfh panel. Antibodies were incubated with cells for 30 min at room temperature. After surface staining, cells were washed in FACS buffer and fixed using the Cytofix/Cytoperm kit (BD Biosciences) for the Th1 panel and the FoxP3 transcription factor buffer kit (eBioscience) for the Tfh panel, according to the manufacturer's instructions. After fixation, the cells were washed in the appropriate perm buffer and incubated with antibodies against CD3, TNF-α, IFN-γ, and IL-2 for the Th1 panel and CD3, TNF-α, IFN-γ, IL-2, and Bcl6 for the Tfh panel for 1 h at room temperature. After staining, the cells were washed with the appropriate perm buffer, fixed (PBS containing 1% paraformaldehyde) and stored at 4°C until analysis.

For B cell subsets, enumeration of splenocytes before RBC lysis was performed with a Vi-Cell (BD). After RBC lysis (Lonza) for 30 s, cells were stained with Zombie L/D Aqua (BioLegend), according to manufacturer's instructions, and for IgD, CD4, CD8, Gr-1, F4/80, B220, CD138, CD19, IgM, CD38, and PNA for 30 min in PBS with 0.5% BSA. Cells were filtered and immediately subjected to flow analysis. GC B cells were determined by gating for IgD$^-$, DUMP$^-$ (CD4$^-$, CD8$^-$, Gr-1$^-$, and F4/80$^-$), B220$^+$, CD138$^-$, CD19$^+$, IgM$^-$, CD38$^-$, and PNA$^+$ cells. Plasma cells were determined by gating for IgD$^-$, DUMP$^-$, and CD138$^+$ cells. Specific population counts were determined by multiplying the percentage of live cells according to FACS with total live cell counts.

Monkeys
Detection of Env-specific Tfh cells from lymph nodes was performed as described previously (Havenar-Daughton et al., 2016). Briefly, rhesus macaque lymph node cells (10^6 cells) were cultured for 18 h at 37°C with 5% CO$_2$ and no exogenous stimulation or with CH505 Env stimulation (5 µg/ml CH505 gp140 Env protein and 0.5 µg/ml of each 15-mer peptide of a peptide pool spanning CH505 Env). SEB-stimulated (0.5 µg/ml; List Biological Laboratories) and unstimulated samples for each animal were included. After stimulation, cells were labeled with antibodies to the following surface antigens: CD3, CD4, and CXCR5-biotin, followed by detection with streptavidin-PE-Cy7, PD-1, OX40, and CD25.

Flow cytometry and cell sorting
Mice
Splenocytes were analyzed on a modified LSR II flow cytometer (BD Biosciences). 100,000 events were collected per specimen. After the gates for each function were created, the Boolean gate platform was used to create the full array of possible combinations, equating to seven response patterns when testing three functions. Data were expressed by first subtracting the percentages from the unstimulated, stained cells from each Env or HA peptide pool and then summing the four or two pools, respectively.

Cells were sorted on an Aria II (BD Biosciences) cell sorter. Splenocytes were prepared, as described for B cells, and 20,000 Tfh cells (TCRβ$^+$CD19$^-$CD4$^+$CD62L$^-$CXCR5$^+$PD-1$^+$) were sorted directly into RNA lysis buffer (Qiagen), supplemented with 2-mercaptoethanol. Samples were stored at –80°C until RNA extraction.

Monkeys
Cells from lymph nodes were analyzed on an LSR II flow cytometer (BD Biosciences). The frequency of Env-specific Tfh cells was calculated by subtracting the frequency of OX40$^+$CD25$^+$ cells in unstimulated cultures from that in Env-stimulated cultures.

RNA isolation and quantitative real-time PCR
RNA was extracted with the RNeasy kit (QIAGEN) and reverse transcribed with SuperScript II Reverse transcription (Invitrogen), according to the manufacturer's protocols. cDNA was amplified with TaqMan Universal Master Mix (Applied Biosystems) and Taqman primers and probes for IL-4, IL-21, IFN-γ, and GAPDH genes (Applied Biosystems). Real-time PCR was performed with an ABI 7300 (Applied Biosystems). Relative expression ($\Delta\Delta C_t$) was calculated using *Gapdh* expression as an endogenous control for cells that were sorted by FACS. Probes used were *Il4* (Mm00445260_m1), *Ifnγ* (Mm00801778_m1), *Il21* (Mm00517640_m1), and *Gapdh* (Mm99999915_g1).

Biolayer interferometry
Biolayer interferometry on an Octet red platform (ForteBio) was used to measure binding kinetics of purified HA to serum antibodies. Briefly, mouse serum samples were diluted 1:100 in assay buffer (PBS, pH 7.4, supplemented with 1% BSA, 0.03% Tween 20, and 0.01% azide) and IgG was captured directly on anti–mouse IgG-coated fiberoptic tips (AMC IgG capture dip and read biosensors). After an extended equilibration for 10 min in assay buffer, a series of tips on which mouse IgG had been immobilized from a diluted serum sample was submerged in assay buffer containing a twofold dilution series of purified HA (starting at 31.25 nM) for 200 s. Those tips were then transferred to wells containing only assay buffer to monitor HA dissociation for 900 s. Biosensor regeneration was accomplished between kinetic determinations by eluting bound IgG and IgG:HA complexes in 1 M glycine at a pH of 2.5, followed by reequilibration in assay buffer. All determinations were performed at 30°C with an instrument shake speed of 1,000 rpm with an independent dilution series of purified HA for each serum sample. After blank reference subtraction, binding curves were aligned to equilibration and Savitzky-Golay smoothing was applied. Kinetic curves were globally fit using the

Pardi et al.
Modified mRNA vaccines induce Tfh and GC B cells

Journal of Experimental Medicine
https://doi.org/10.1084/jem.20171450

1585

simplest 1:1 model of binding to derive affinity constants for each interaction (ForteBio Octet Data Analysis 7.1).

Bioluminescence imaging studies
Bioluminescence imaging was performed with an IVIS Spectrum imaging system (Caliper Life Sciences). Mice were administered D-luciferin (Regis Technologies) at a dose of 150 mg/kg i.p. Mice were anesthetized after receiving D-luciferin in a chamber with 3% isoflurane (Piramal Healthcare Limited) and were placed on the imaging platform while being maintained on 2% isoflurane via a nose cone. Mice were imaged at 5 min after administration of D-luciferin using an exposure time of 5 s or longer to ensure that the signal acquired was within the effective detection range (above the noise levels and below charge-coupled device saturation limit). Bioluminescence values were quantified by measuring photon flux (photons/second) in the region of interest, where the bioluminescence signal emanated, using the Living IMAGE Software provided by Caliper.

Mathematical and statistical analyses
Statistical analyses were performed with Excel (Microsoft), Prism 5.0f (GraphPad Software), PESTLE 1.7, SPICE 5.35, and SAS (version 9.4; SAS Institute) software. Data were compared with a Student's t test; one-way or two-way ANOVA, corrected for multiple comparisons (Bonferroni method); and the Kruskal-Wallis test. Area under the curve calculations were performed using the equation $AUC = \sum (t_{i+1} - t_i)/2 \times (C_i + C_{i+1})$, where t_i is the starting time point, t_{i+1} is the finishing time point, C_i is the starting value, and C_{i+1} is the finishing value for each measurement over time.

Online supplemental material
Fig. S1 shows representative flow cytometry plots for the various mouse experiments. Fig. S2 shows anti–gp120 IgG titers in mice after two immunizations with HIV-1 Env m1Ψ-mRNA-LNPs. Fig. S3 shows splenic GC B cell and plasma cell numbers in mice after a single immunization with various influenza virus vaccine platforms. Fig. S4 demonstrates that m1Ψ-mRNA–LNP immunization results in potent increases in apparent affinity of anti–HA antibodies in mice. Fig. S5 shows representative flow cytometry plots for nonhuman primate experiments.

References
Alberer, M., U. Gnad-Vogt, H.S. Hong, K.T. Mehr, L. Backert, G. Finak, R. Gottardo, M.A. Bica, A. Garofano, S.D. Koch, et al. 2017. Safety and immunogenicity of a mRNA rabies vaccine in healthy adults: an open-label, non-randomised, prospective, first-in-human phase 1 clinical trial. *Lancet*. 390:1511–1520. https://doi.org/10.1016/S0140-6736(17)31665-3

Andries, O., S. Mc Cafferty, S.C. De Smedt, R. Weiss, N.N. Sanders, and T. Kitada. 2015. N¹-methylpseudouridine-incorporated mRNA outperforms pseudouridine-incorporated mRNA by providing enhanced protein expression and reduced immunogenicity in mammalian cell lines and mice. *J. Control. Release*. 217:337–344. https://doi.org/10.1016/j.jconrel.2015.08.051

Bahl, K., J.J. Senn, O. Yuzhakov, A. Bulychev, L.A. Brito, K.J. Hassett, M.E. Laska, M. Smith, Ö. Almarsson, J. Thompson, et al. 2017. Preclinical and Clinical Demonstration of Immunogenicity by mRNA Vaccines against

H10N8 and H7N9 Influenza Viruses. *Mol. Ther.* 25:1316–1327. https://doi.org/10.1016/j.ymthe.2017.03.035

Chen, J., R.R. Pompano, F.W. Santiago, L. Maillat, R. Sciammas, T. Sun, H. Han, D.J. Topham, A.S. Chong, and J.H. Collier. 2013. The use of self-adjuvanting nanofiber vaccines to elicit high-affinity B cell responses to peptide antigens without inflammation. *Biomaterials.* 34:8776–8785. https://doi.org/10.1016/j.biomaterials.2013.07.063

Chowdhury, A., P.M. Del Rio Estrada, G.K. Tharp, R.P. Trible, R.R. Amara, A. Chahroudi, G. Reyes-Teran, S.E. Bosinger, and G. Silvestri. 2015. Decreased T Follicular Regulatory Cell/T Follicular Helper Cell (TFH) in Simian Immunodeficiency Virus-Infected Rhesus Macaques May Contribute to Accumulation of TFH in Chronic Infection. *J. Immunol.* 195:3237–3247. https://doi.org/10.4049/jimmunol.1402701

Clausen, B.E., and P. Stoitzner. 2015. Functional Specialization of Skin Dendritic Cell Subsets in Regulating T Cell Responses. *Front. Immunol.* 6:534. https://doi.org/10.3389/fimmu.2015.00534

Crotty, S. 2014. T follicular helper cell differentiation, function, and roles in disease. *Immunity.* 41:529–542. https://doi.org/10.1016/j.immuni.2014.10.004

Cucak, H., U. Yrlid, B. Reizis, U. Kalinke, and B. Johansson-Lindbom. 2009. Type I interferon signaling in dendritic cells stimulates the development of lymph-node-resident T follicular helper cells. *Immunity.* 31:491–501. https://doi.org/10.1016/j.immuni.2009.07.005

Fera, D., A.G. Schmidt, B.F. Haynes, F. Gao, H.X. Liao, T.B. Kepler, and S.C. Harrison. 2014. Affinity maturation in an HIV broadly neutralizing B-cell lineage through reorientation of variable domains. *Proc. Natl. Acad. Sci. USA.* 111:10275–10280. https://doi.org/10.1073/pnas.1409954111

Gao, F., R.M. Scearce, S.M. Alam, B. Hora, S. Xia, J.E. Hohm, R.J. Parks, D.F. Ogburn, G.D. Tomaras, E. Park, et al. 2009. Cross-reactive monoclonal antibodies to multiple HIV-1 subtype and SIVcpz envelope glycoproteins. *Virology.* 394:91–98. https://doi.org/10.1016/j.virol.2009.07.041

Guo, W., B. Cleveland, T.M. Davenport, K.K. Lee, and S.L. Hu. 2013. Purification of recombinant vaccinia virus-expressed monomeric HIV-1 gp120 to apparent homogeneity. *Protein Expr. Purif.* 90:34–39. https://doi.org/10.1016/j.pep.2013.04.009

Hannoun, C., F. Megas, and J. Piercy. 2004. Immunogenicity and protective efficacy of influenza vaccination. *Virus Res.* 103:133–138. https://doi.org/10.1016/j.virusres.2004.02.025

Havenar-Daughton, C., S.M. Reiss, D.G. Carnathan, J.E. Wu, K. Kendric, A. Torrents de la Peña, S.P. Kasturi, J.M. Dan, M. Bothwell, R.W. Sanders, et al. 2016. Cytokine-Independent Detection of Antigen-Specific Germinal Center T Follicular Helper Cells in Immunized Nonhuman Primates Using a Live Cell Activation-Induced Marker Technique. *J. Immunol.* 197:994–1002. https://doi.org/10.4049/jimmunol.1600320

Havenar-Daughton, C., J.H. Lee, and S. Crotty. 2017. Tfh cells and HIV bnAbs, an immunodominance model of the HIV neutralizing antibody generation problem. *Immunol. Rev.* 275:49–61. https://doi.org/10.1111/imr.12512

Jayaraman, M., S.M. Ansell, B.L. Mui, Y.K. Tam, J. Chen, X. Du, D. Butler, L. Eltepu, S. Matsuda, J.K. Narayanannair, et al. 2012. Maximizing the potency of siRNA lipid nanoparticles for hepatic gene silencing in vivo. *Angew. Chem. Int. Ed. Engl.* 51:8529–8533. https://doi.org/10.1002/anie.201203263

Kallen, K.J., R. Heidenreich, M. Schnee, B. Petsch, T. Schlake, A. Thess, P. Baumhof, B. Scheel, S.D. Koch, and M. Fotin-Mleczek. 2013. A novel, disruptive vaccination technology: self-adjuvanted RNActive(®) vaccines. *Hum. Vaccin. Immunother.* 9:2263–2276. https://doi.org/10.4161/hv.25181

Karikó, K., H. Muramatsu, F.A. Welsh, J. Ludwig, H. Kato, S. Akira, and D. Weissman. 2008. Incorporation of pseudouridine into mRNA yields superior nonimmunogenic vector with increased translational capacity and biological stability. *Mol. Ther.* 16:1833–1840. https://doi.org/10.1038/mt.2008.200

Karikó, K., H. Muramatsu, J. Ludwig, and D. Weissman. 2011. Generating the optimal mRNA for therapy: HPLC purification eliminates immune activation and improves translation of nucleoside-modified, protein-encoding mRNA. *Nucleic Acids Res.* 39:e142. https://doi.org/10.1093/nar/gkr695

Kato, Y., A. Zaid, G.M. Davey, S.N. Mueller, S.L. Nutt, D. Zotos, D.M. Tarlinton, K. Shortman, M.H. Lahoud, W.R. Heath, and I. Caminschi. 2015. Targeting Antigen to Clec9A Primes Follicular Th Cell Memory Responses Capable of Robust Recall. *J. Immunol.* 195:1006–1014. https://doi.org/10.4049/jimmunol.1500767

Kauffman, K.J., M.J. Webber, and D.G. Anderson. 2016. Materials for non-viral intracellular delivery of messenger RNA therapeutics. *J. Control. Release.* 240:227–234. https://doi.org/10.1016/j.jconrel.2015.12.032

Krammer, F. 2016. Novel universal influenza virus vaccine approaches. *Curr. Opin. Virol.* 17:95–103. https://doi.org/10.1016/j.coviro.2016.02.002

Kwong, P.D., and J.R. Mascola. 2012. Human antibodies that neutralize HIV-1: identification, structures, and B cell ontogenies. *Immunity.* 37:412–425. https://doi.org/10.1016/j.immuni.2012.08.012

Kwong, P.D., J.R. Mascola, and G.J. Nabel. 2013. Broadly neutralizing antibodies and the search for an HIV-1 vaccine: the end of the beginning. *Nat. Rev. Immunol.* 13:693–701. https://doi.org/10.1038/nri3516

Lahoud, M.H., F. Ahmet, S. Kitsoulis, S.S. Wan, D. Vremec, C.N. Lee, B. Phipson, W. Shi, G.K. Smyth, A.M. Lew, et al. 2011. Targeting antigen to mouse dendritic cells via Clec9A induces potent CD4 T cell responses biased toward a follicular helper phenotype. *J. Immunol.* 187:842–850. https://doi.org/10.4049/jimmunol.1101176

Liang, F., G. Lindgren, A. Lin, E.A. Thompson, S. Ols, J. Röhss, S. John, K. Hassett, O. Yuzhakov, K. Bahl, et al. 2017. Efficient Targeting and Activation of Antigen-Presenting Cells In Vivo after Modified mRNA Vaccine Administration in Rhesus Macaques. *Mol. Ther.* 25:2635–2647. https://doi.org/10.1016/j.ymthe.2017.08.006

Lindgren, G., S. Ols, F. Liang, E.A. Thompson, A. Lin, F. Hellgren, K. Bahl, S. John, O. Yuzhakov, K.J. Hassett, et al. 2017. Induction of Robust B Cell Responses after Influenza mRNA Vaccination Is Accompanied by Circulating Hemagglutinin-Specific ICOS+ PD-1+ CXCR3+ T Follicular Helper Cells. *Front. Immunol.* 8:1539. https://doi.org/10.3389/fimmu.2017.01539

Locci, M., J.E. Wu, F. Arumemi, Z. Mikulski, C. Dahlberg, A.T. Miller, and S. Crotty. 2016. Activin A programs the differentiation of human TFH cells. *Nat. Immunol.* 17:976–984. https://doi.org/10.1038/ni.3494

Lutz, J., S. Lazzaro, M. Habbeddine, K.E. Schmidt, P. Baumhof, B.L. Mui, Y.K. Tam, T.D. Madden, M.J. Hope, R. Heidenreich, and M. Fotin-Mleczek. 2017. Unmodified mRNA in LNPs constitutes a competitive technology for prophylactic vaccines. *NPJ Vaccines.* 2:29. https://doi.org/10.1038/s41541-017-0032-6

Maier, M.A., M. Jayaraman, S. Matsuda, J. Liu, S. Barros, W. Querbes, Y.K. Tam, S.M. Ansell, V. Kumar, J. Qin, et al. 2013. Biodegradable lipids enabling rapidly eliminated lipid nanoparticles for systemic delivery of RNAi therapeutics. *Mol. Ther.* 21:1570–1578. https://doi.org/10.1038/mt.2013.124

Martinon, F., S. Krishnan, G. Lenzen, R. Magné, E. Gomard, J.G. Guillet, J.P. Lévy, and P. Meulien. 1993. Induction of virus-specific cytotoxic T lymphocytes in vivo by liposome-entrapped mRNA. *Eur. J. Immunol.* 23:1719–1722. https://doi.org/10.1002/eji.1830230749

Martins, K.A., J.T. Steffens, S.A. van Tongeren, J.B. Wells, A.A. Bergeron, S.P. Dickson, J.M. Dye, A.M. Salazar, and S. Bavari. 2014. Toll-like receptor agonist augments virus-like particle-mediated protection from Ebola virus with transient immune activation. *PLoS One.* 9:e89735. https://doi.org/10.1371/journal.pone.0089735

Mastelic Gavillet, B., C.S. Eberhardt, F. Auderset, F. Castellino, A. Seubert, J.S. Tregoning, P.H. Lambert, E. de Gregorio, G. Del Giudice, and C.A. Siegrist. 2015. MF59 Mediates Its B Cell Adjuvanticity by Promoting T Follicular Helper Cells and Thus Germinal Center Responses in Adult and Early Life. *J. Immunol.* 194:4836–4845. https://doi.org/10.4049/jimmunol.1402071

Meissner, E.G., K.M. Duus, F. Gao, X.F. Yu, and L. Su. 2004. Characterization of a thymus-tropic HIV-1 isolate from a rapid progressor: role of the envelope. *Virology.* 328:74–88. https://doi.org/10.1016/j.virol.2004.07.019

Montefiori, D.C. 2009. Measuring HIV neutralization in a luciferase reporter gene assay. *Methods Mol. Biol.* 485:395–405. https://doi.org/10.1007/978-1-59745-170-3_26

Montefiori, D.C., C. Karnasuta, Y. Huang, H. Ahmed, P. Gilbert, M.S. de Souza, R. McLinden, S. Tovanabutra, A. Laurence-Chenine, E. Sanders-Buell, et al. 2012. Magnitude and breadth of the neutralizing antibody response in the RV144 and Vax003 HIV-1 vaccine efficacy trials. *J. Infect. Dis.* 206:431–441. https://doi.org/10.1093/infdis/jis367

Morrissey, D.V., J.A. Lockridge, L. Shaw, K. Blanchard, K. Jensen, W. Breen, K. Hartsough, L. Machemer, S. Radka, V. Jadhav, et al. 2005. Potent and persistent in vivo anti-HBV activity of chemically modified siRNAs. *Nat. Biotechnol.* 23:1002–1007. https://doi.org/10.1038/nbt1122

Pardi, N., H. Muramatsu, D. Weissman, and K. Karikó. 2013. In vitro transcription of long RNA containing modified nucleosides. *Methods Mol. Biol.* 969:29–42. https://doi.org/10.1007/978-1-62703-260-5_2

Pardi, N., S. Tuyishime, H. Muramatsu, K. Kariko, B.L. Mui, Y.K. Tam, T.D. Madden, M.J. Hope, and D. Weissman. 2015. Expression kinetics of nucleoside-modified mRNA delivered in lipid nanoparticles to mice by various routes. *J. Control. Release.* 217:345–351. https://doi.org/10.1016/j.jconrel.2015.08.007

Pardi, N., M.J. Hogan, R.S. Pelc, H. Muramatsu, H. Andersen, C.R. DeMaso, K.A. Dowd, L.L. Sutherland, R.M. Scearce, R. Parks, et al. 2017. Zika virus protection by a single low-dose nucleoside-modified mRNA vaccination. *Nature.* 543:248–251. https://doi.org/10.1038/nature21428

Pardi, N., M.J. Hogan, F.W. Porter, and D. Weissman. 2018. mRNA vaccines - a new era in vaccinology. *Nat. Rev. Drug Discov.* 17:261–279. https://doi.org/10.1038/nrd.2017.243

Pauthner, M., C. Havenar-Daughton, D. Sok, J.P. Nkolola, R. Bastidas, A.V. Boopathy, D.G. Carnathan, A. Chandrashekar, K.M. Cirelli, C.A. Cottrell, et al. 2017. Elicitation of robust tier 2 neutralizing antibody responses in nonhuman primates by HIV envelope trimer immunization using optimized approaches. *Immunity.* 46:1073–1088.

Quan, F.S., Y.T. Lee, K.H. Kim, M.C. Kim, and S.M. Kang. 2016. Progress in developing virus-like particle influenza vaccines. *Expert Rev. Vaccines.* 15:1281–1293. https://doi.org/10.1080/14760584.2016.1175942

Richner, J.M., S. Himansu, K.A. Dowd, S.L. Butler, V. Salazar, J.M. Fox, J.G. Julander, W.W. Tang, S. Shresta, T.C. Pierson, et al. 2017. Modified mRNA Vaccines Protect against Zika Virus Infection. *Cell.* 168:1114–1125.

Riteau, N., A.J. Radtke, K. Shenderov, L. Mittereder, S.D. Oland, S. Hieny, D. Jankovic, and A. Sher. 2016. Water-in-Oil-Only Adjuvants Selectively Promote T Follicular Helper Cell Polarization through a Type I IFN and IL-6-Dependent Pathway. *J. Immunol.* 197:3884–3893. https://doi.org/10.4049/jimmunol.1600883

Schnee, M., A.B. Vogel, D. Voss, B. Petsch, P. Baumhof, T. Kramps, and L. Stitz. 2016. An mRNA Vaccine Encoding Rabies Virus Glycoprotein Induces Protection against Lethal Infection in Mice and Correlates of Protection in Adult and Newborn Pigs. *PLoS Negl. Trop. Dis.* 10:e0004746. https://doi.org/10.1371/journal.pntd.0004746

Sultan, H., V.I. Fesenkova, D. Addis, A.E. Fan, T. Kumai, J. Wu, A.M. Salazar, and E. Celis. 2017. Designing therapeutic cancer vaccines by mimicking viral infections. *Cancer Immunol. Immunother.* 66:203–213. https://doi.org/10.1007/s00262-016-1834-5

Tam, H.H., M.B. Melo, M. Kang, J.M. Pelet, V.M. Ruda, M.H. Foley, J.K. Hu, S. Kumari, J. Crampton, A.D. Baldeon, et al. 2016. Sustained antigen availability during germinal center initiation enhances antibody responses to vaccination. *Proc. Natl. Acad. Sci. USA.* 113:E6639–E6648. https://doi.org/10.1073/pnas.1606050113

Thess, A., S. Grund, B.L. Mui, M.J. Hope, P. Baumhof, M. Fotin-Mleczek, and T. Schlake. 2015. Sequence-engineered mRNA Without Chemical Nucleoside Modifications Enables an Effective Protein Therapy in Large Animals. *Mol. Ther.* 23:1456–1464. https://doi.org/10.1038/mt.2015.103

Victora, G.D., and M.C. Nussenzweig. 2012. Germinal centers. *Annu. Rev. Immunol.* 30:429–457. https://doi.org/10.1146/annurev-immunol-020711-075032

Victora, G.D., and P.C. Wilson. 2015. Germinal center selection and the antibody response to influenza. *Cell.* 163:545–548. https://doi.org/10.1016/j.cell.2015.10.004

Villarreal, D.O., K.T. Talbott, D.K. Choo, D.J. Shedlock, and D.B. Weiner. 2013. Synthetic DNA vaccine strategies against persistent viral infections. *Expert Rev. Vaccines.* 12:537–554. https://doi.org/10.1586/erv.13.33

Wang, C., P. Liu, Y. Zhuang, P. Li, B. Jiang, H. Pan, L. Liu, L. Cai, and Y. Ma. 2014. Lymphatic-targeted cationic liposomes: a robust vaccine adjuvant for promoting long-term immunological memory. *Vaccine.* 32:5475–5483. https://doi.org/10.1016/j.vaccine.2014.07.081

Weissman, D., N. Pardi, H. Muramatsu, and K. Karikó. 2013. HPLC purification of in vitro transcribed long RNA. *Methods Mol. Biol.* 969:43–54. https://doi.org/10.1007/978-1-62703-260-5_3

Yamamoto, T., R.M. Lynch, R. Gautam, R. Matus-Nicodemos, S.D. Schmidt, K.L. Boswell, S. Darko, P. Wong, Z. Sheng, C. Petrovas, et al. 2015. Quality and quantity of TFH cells are critical for broad antibody development in SHIVAD8 infection. *Sci. Transl. Med.* 7:298ra120. https://doi.org/10.1126/scitranslmed.aab3964

Yao, C., S.M. Zurawski, E.S. Jarrett, B. Chicoine, J. Crabtree, E.J. Peterson, G. Zurawski, D.H. Kaplan, and B.Z. Igyarto. 2015. Skin dendritic cells induce follicular helper T cells and protective humoral immune responses. *J. Allergy Clin. Immunol.* 136:1387–1397.